# THESIS APPROVAL

## GRADUATE SCHOOL, KASETSART UNIVERSITY

Master of Science (Chemistry)

**DEGREE**

| Chemistry | Chemistry |
|---|---|
| **FIELD** | **DEPARTMENT** |

**TITLE:** Density Functional Theory Evidence for an Electron Hopping Process in Single-Walled Carbon Nanotube-Mediated Redox Reactions

**NAME:** Mr. Teeranan Nongnual

**THIS THESIS HAS BEEN ACCEPTED BY**

**THESIS ADVISOR**

( Mr. Somkiat Nokbin, Ph.D. )

**THESIS CO-ADVISOR**

( Professor Jumras Limtrakul, Ph.D. )

**THESIS CO-ADVISOR**

( Mr. Pipat Khongpracha, Ph.D. )

**DEPARTMENT HEAD**

( Associate Professor Supa Hannongbua, Dr.rer.nat. )

**APPROVED BY THE GRADUATE SCHOOL ON** _____

**DEAN**

( Associate Professor Gunjana Theeragool, D.Agr. )

THESIS

# DENSITY FUNCTIONAL THEORY EVIDENCE FOR AN ELECTRON HOPPING PROCESS IN SINGLE-WALLED CARBON NANOTUBE-MEDIATED REDOX REACTIONS

TEERANAN NONGNUAL

A Thesis Submitted in Partial Fulfillment of
the Requirements for the Degree of
Masterof Science (Chemistry)
Graduate School, Kasetsart University
2010

Teeranan Nongnual 2010: Density Functional Theory Evidence for an Electron Hopping Process in Single-Walled Carbon Nanotube-Mediated Redox Reactions. Master of Science (Chemistry), Major Field: Chemistry, Department of Chemistry. Thesis Advisor: Mr. Somkiat Nokbin, Ph.D. 48 pages.

The electron hopping mechanism in the single-walled carbon nanotube (SWCNT)-mediated redox reaction between anthraquinonyl ($AQH_2$-) and 4-arylhydroxyl amine (4AHA-) groups was studied by density functional theory calculations. The (8,0) SWCNT was used to mimic the real system of interest. It was found that electrons from the oxidized $AQH_2$ group can be transferred to the oxidizing 4AHA group, at the other end of the nanotube, by a hopping process through the mediating SWCNT. Disparity of electron densities ascribable to non-localized electrons confirmed this finding. The disparity, partial electron density difference, and Hirshfeld partial charges analyses shown that the SWCNT can hold 87% of the extra electron density of the hypothetical negative intermediate produced from the oxidation of the $AQH_2$ process. Chemical attachments of these two redox reagents to the SWCNT also caused new impurity states within the band gap, thereby giving more metallic characteristics to the system. These findings provided a detailed understanding of the electron hopping process and agree well with a previous experimental study.

/ /

Student's signature Thesis Advisor's signature

# ACKNOWLEDGEMENTS

I was very pleased to get the special opportunity in my graduate study at one of the best physical chemistry and nanotechnology laboratory in Thailand under a well-known professor, Prof. Dr. Jumras Limtrakul. The idea of my project was initiated by his basic scientific curiosity about an online article focusing on carbon nanotube-mediated redox reactions. After that, he thoroughly took care of every step of my works, pushing me to get all jobs done in time with quite high quality outputs. I would like to thank him so much and extend my special thank to my fresh advisors, Dr. Somkiat Nokbin and Dr. Pipat Khongpracha. They gave insightful comments and reviewed my work. In addition, my deep thanks go to Prof. Philippe Anthony Bopp who adjusted any grammatical and chemical flaws in the manuscript. Therefore, my work was achieved as expected and my chemistry skill was consolidated, leading to the Master's degree in Chemistry at Kasetsart University and also brightening my upcoming study and my life. Moreover, I would like to thank my thesis committee, Dr. Piti Treesakul who is the representative of the Graduate School of Kasetsart University for his helpful comments and suggestions.

I am also grateful for the participation of many members of the Laboratory for Computational and Applied Chemistry (LCAC), Kasetsart University. In addition, this work was supported in part by grants from the National Science and Technology Development Agency and NANOTEC Center of Excellence (2009 NSTDA Chair Professor), Kasetsart University Research and Development Institute (KURDI), the Thailand Research Fund (TRF), and the Commission of Higher Education, Ministry of Education under Postgraduate Education and Research Programs in Petroleum and Petrochemicals and Advanced Materials and the Development and Promotion of Science and Technology Talents Project (DPST). The Kasetsart University Graduate School is also acknowledged. The computational calculations are supported by the Thai National Grid Center (TNGC) under the SIPA.

Teeranan Nongnual

March 2010

# TABLE OF CONTENTS

**Page**

# LIST OF TABLES

# LIST OF FIGURES

# LIST OF FIGURES (Continued)

# LIST OF ABBREVIATIONS

| | | |
|---|---|---|
| BLYP | = | Becke's exchange and Lee, Yang, and Parr's correlation functional |
| CNT | = | Carbon nanotube |
| 4AA | = | 4-Arylamine |
| 4AHA | = | 4-Arylhydroxyl amine |
| AQ | = | Anthraquinonyl |
| $AQH_2$ | = | Anthraquinolyl |
| *calc* | = | Calculation data |
| CV | = | Cyclic voltammetry |
| DFT | = | Density functional theory |
| DNP | = | All-electron Double Numerial basis set with Polarized function |
| *E*gap | = | Energy gap |
| eV | = | Electron volt |
| *expt* | = | Experimental data |
| GGA | = | Generalized Gradient Approximation |
| HOMO | = | Highest Occupied Molecular Orbital |
| *int-1-a* | = | Intermediate-1-a structure |
| *int-1-b* | = | Intermediate-1-b structure |
| *int-2* | = | Intermediate-2 structure |
| *int-3* | = | Intermediate-3 structure |
| kcal | = | Kilocalories |
| LUMO | = | Lowest Unoccupied Molecular Orbital |
| MO | = | Molecular Orbital |
| MWCNT | = | Multi-walled carbon nanotube |
| NP | = | 4-Nitrophenyl |
| Ph | = | Phenyl group |
| SWCNT | = | Single-walled carbon nanotube |

# DENSITY FUNCTIONAL THEORY EVIDENCE FOR AN ELECTRON HOPPING PROCESS IN SINGLE-WALLED CARBON NANOTUBE-MEDIATED REDOX REACTIONS

## INTRODUCTION

Among all nanoscale morphologies of carbon, multi-walled carbon nanotubes (MWCNTs) were first observed under transmission electron microscopy (TEM) by Iijima in 1991 (Iijima, 1991). After that, single-walled carbon nanotubes (SWCNTs) were produced independently by Iijima (Iijima *et al.*, 1993) and Bethune (Bethune *et al.*, 1993) in 1993. Since these discoveries of low-dimensional carbon nanostructures, carbon nanotubes (CNTs) have attracted much interest in modern nanoscience and nanotechnology due to their novel and structure-dependent properties. Over the years, the physical and chemical properties of CNTs have been well-documented with more and more sophisticated methods. The novel properties of these CNTs allowed their application as nanoelectronic devices (Tans *et al.*, 1998), sensors (Kong *et al.*, 2000), field emission sources (de Heer *et al.*, 1995), and composite materials (Baughman *et al.*, 2002). The CNTs also functioned as nanowires to transport electrons between an electrode and electroactive proteins chemically attached on each end of the tube (Gooding *et al.*, 2003). The transport distances, controlling the rate of electron transfer, were larger than 150 nm from the enzymatic active center to the electrode (Patolsky *et al.*, 2004).

The chemical functionalization reactions for CNTs were categorized into three methods, which are: direct attachment to the graphitic surface, ester linkage, and covalent binding using diazonium reagents with high selectivity. The diazonium media method was further developed by Compton's group to initiate chemisorptions of aryl diazonium salts by direct reduction with hypophosphorous acid in the presence of carbon powder (Pandurangappa *et al.*, 2002; Wildgoose *et al.*, 2003; Leventis *et al.*, 2004). The method was further extended to the application on MWCNTs with

anthraquinone-1-diazonium chloride and 4-nitrobenzenediazonium tetrafluoroborate, resulting in the synthesis of 1-anthraquinonyl-MWCNTs (AQ-MWCNTs) and 4-nitrophenyl-MWCNTs (NB-MWCNTs) (Charles G. R. Heald, 2004).

Recently, Wong and coworkers (Wong *et al.*, 2008) reported a redox reaction on the same MWCNT for the first time. This MWCNT was functionalized with two redox-active species, directly attached by the diazonium salt method. The 4-arylhydroxyl amine (4AHA) and $AQH_2$ species were generated in the first oxidation cycle from $NO_2$–$C_6H_4$–MWCNT and AQ–MWCNT, respectively. This redox reaction consisted of a reversible oxidation and an irreversible reduction; it was studied by the cyclic voltammetry technique. These authors proposed a redox reaction mechanism where $AQH_2$ is the oxidizing agent with the oxidation peak at $E_a$ = –0.385 V while NHOH–$C_6H_4$ is the reducing group gradually lessening the peak currents of the oxidation peak at $E_a$ = 0.125 V.

$$AQH_2 - \mathbf{MWCNT} - C_6H_4 - NHOH \rightarrow AQ - \mathbf{MWCNT} - C_6H_4 - NH_2 + H_2O$$

The pathway of electron transfer from $AQH_2$ to the 4-arylhydroxyl amine group was investigated to determine whether it was via intermolecular electron tunneling between reagents or by electron hopping via the CNT. The hopping was proposed to be more favorable because of the shorter distance through the tube compared to a process through the solvent. This phenomenon was unique for both oxidizing and reducing groups confined to the same CNT.

Here, we reported a theoretical study on the possible processes of electron hopping between two redox reagents functionalized on the same CNT. The mediating MWCNT (in the real system) was simplified to a semiconducting SWCNT for computational efficiency. Periodic calculations were performed to obtain computed electronic properties as realistic as possible. Although time-dependent calculations can yield more details about the electron transfer, such calculations are not practicable

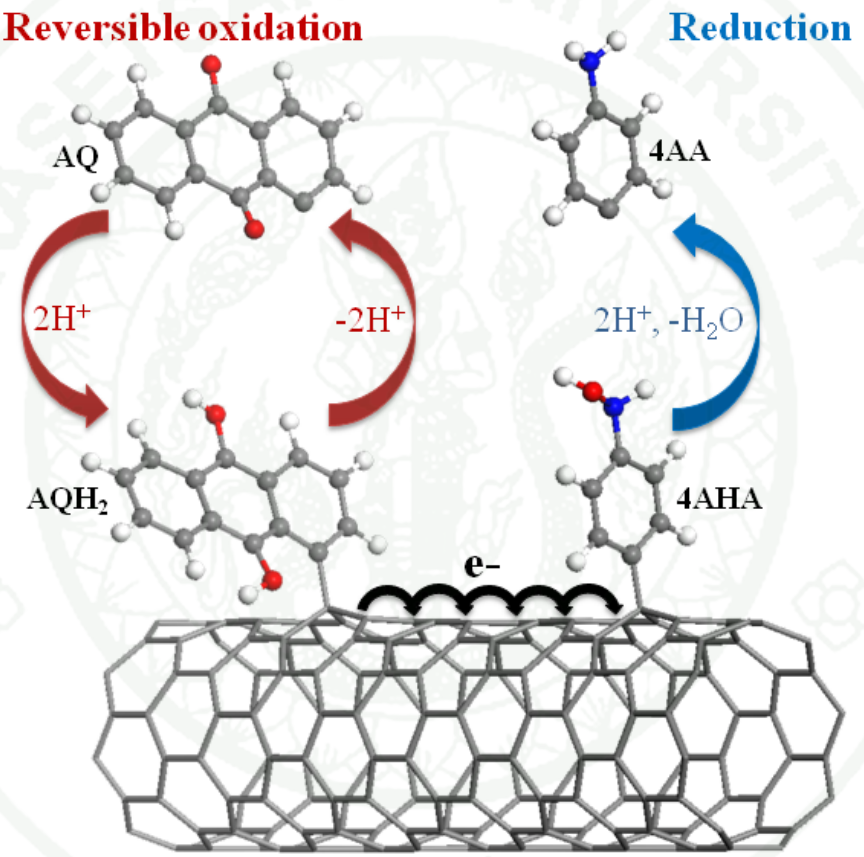

**SWCNT**–4AHA, terminated at AQ–**SWCNT**–4AA, was proposed. It can be subdivided into a reversible oxidation and an irreversible reduction (see Figure 1), where 4-arylamine is noted as 4AA.

Total reaction:

$AQH_2$ – **SWCNT** – 4AHA

$\rightarrow$ AQ – **SWCNT** – 4AA + $H_2O$

Oxidation:

$AQH_2$ – **SWCNT** – 4AHA

$\leftrightarrow$ AQ – **SWCNT** – 4AHA + $2H^+$ + $2e^-$

Reduction:

AQ – **SWCNT** – 4AHA + $2H^+$ + $2e^-$

$\rightarrow$ AQ – **SWCNT** – 4AA + $H_2O$

# OBJECTIVES

1. To investigate the structures, electronic properties and reaction mechanisms of the anthraquinonyl and 4-arylhydroxyl amine redox reaction mediated carbon nanotube by the periodic DFT calculations.

2. To study and confirm the electron transfer process between two redox species via carbon nanotube with the previous experimental studies.

# LITERATURE REVIEW

According to one of original researches focusing on electron transport properties of the carbon nanotubes, Gooding (Gooding *et al.*, 2003) reported in 2003 that the carbon nanotubes functioning as nanowires can transport electrons between an electrode and electroactive proteins chemically attached on each end of the tube. This is important in the understanding of the redox properties of proteins and also in the development of enzyme biosensors without mediators. With the advantages of their electrocatalytic properties and their small size, carbon nanotubes are attractive materials in bioelectrochemistry, especially as the possibility exists to bring the nanotubes close to the redox centers of the proteins. From the perspective of electron-transfer properties, the open ends of carbon nanotubes have been likened to edge planes of highly oriented pyrolytic graphite (HOPG), while the walls were suggested to have properties similar to those of the basal planes of HOPG. In the results, the multi-walled carbon nanotubes have shown good communication with redox proteins where not only the redox active center was close to the surface of the protein, such as cytochrome *c*, azurin, and horseradish peroxidase, but also it was embedded deep within the glycoprotein such as glucose oxidase. In addition, a strategy for investigating the electron-transfer properties of redox enzymes was presented.

After the electron-transport properties of carbon nanotubes were revealed, the upcoming question was how long of the transport distance. Patolsky (Patolsky *et al.*, 2004) reported this answer concerning their experimental model, which was the enzyme glucose oxidase, GOx, on electrodes by using SWCNTs as electrical connectors between the enzyme redox centers and the electrode. The surface-assembled GOx was electrically contacted to the electrode by means of the SWCNTs, which acted as conductive nanoneedles that electrically wire the enzyme redox-active site to the transducer surface. The effect of the length of the SWCNT controlling the electrical-communication properties between the enzyme redox center and the electrode was discussed. In the results, the SWCNT acted as a nanoconnector that electrically contacted the active site of the enzyme and the electrode. The electrons

were transported along distances greater than 150 nm and the rate of electron transport was controlled by the length of the SWCNTs. These results shown the compatibility of SWCNTs with the preparation of novel biomaterial hybrid systems that may had new fascinating properties.

The covalent-binding method using diazonium reagents with high selectivity is one of chemical functionalization reactions for CNTs. Pandurangappa (Pandurangappa *et al.*, 2002) reported that this diazonium supporting method was developed to initiate chemisorptions of aryl diazonium salts by direct reduction with hypophosphorous acid in the presence of carbon powder. The resulting derivatised carbon was characterized electrochemically showing the behavior expected of a surface bound species. This procedure provided an easy, inexpensive methodology for functionalizing carbon which might find applications in ion-exchange resins or combinatorial chemistry.

The previous study on the electrochemical functionalization of carbon powder was adapted to investigate pH sensing ability of this material. Wildgoose (Wildgoose *et al.*, 2003) reported that a simple pH probe was developed based upon the covalent chemical derivatisation of carbon particles with anthraquinone. The amperometric response of electrodes constructed from this material was examined and shown to produce a Nernstian linear response to pH from 1 to 9, over a range of temperatures from 20 to 70 °C, consistent with a two-electron, two-proton electrochemical process.

The derivatisation of carbon powder electrodes was broadened concerning to reagentless pH sensors. Leventis (Leventis *et al.*, 2004) reported that carbon powder was derivatised with anthracene, azobenzene, diphenylamine, 9,10-diphenylanthracene, methylene blue, 3-nitrofluoranthene, 6-nitrochrysene, 9-nitroanthracene, 9,10-phenanthraquinone (PAQ), thionin, and fast black K (2,5-dimethyloxy-4-[(4-nitrophenyl)azo]benzenediazonium chloride) and separately immobilize the resulting material onto a bppg electrode. The cyclic voltammetry (CV) and square wave voltammetry (SWV) were used to demonstrate that the observed

voltammetric response for each derivatised carbon was consistent with that of an immobilized species and to investigate the effect of pH on the peak potentials of each compound studied over range pH 1–12 and at elevated temperatures up to 70 °C in order to demonstrate the versatility of derivatised carbon electrodes as reagentless pH sensors. Of all the compounds studied it was found that the three compounds exhibiting chemically and electrochemically reversible behavior, namely anthracene, DPA and PAQ, gave the most analytically useful response. A proposed chemical rationalization of each kind of behavior has been put forward and exceptions discussed where they arise. In addition, the results were shown to be in good agreement with theory.

The applications of chemical activation method of covalently derivatising carbon powder, via the chemical reduction of aryl diazonium salts with hypophosphorous acid, were extended by Heald (Charles G. R. Heald, 2004) to include the covalent derivatisation of MWCNTs by anthraquinone-1-diazonium choride and 4-nitrobenzenediazonium tetrafluoroborate. This resulted in the synthesis of 1-anthraquinonyl-MWCNTs (AQ-MWCNTs) and 4-nitrophenyl-MWCNTs (NB-MWCNTs). To the best of our knowledge this represented the first time that CNTs have been derivatised using the chemical, as opposed to the electrochemical, reduction of aryl diazonium salts, thereby demonstrating that this was a useful and versatile method of derivatising carbon materials with a range of aryl diazonium salts. Furthermore the derivatisation of MWCNTs proffers the possibility of sensor miniaturization down to the nanoscale. In addition, it was found that AQ-MWCNTs are insensitive to quite large variations in temperature; therefore, these materials may be used as pH sensors in high-temperature environments. The derivatisation onto the surface of carbon extends the window for using as a pH sensor as the p$K_a$ of the free anthraquinone in solution lower than that of the 1-anthraquinonyl group attached to the suface of MWCNTs.

In order to study the influences of chemical and electronic properties of CNTs, their ability was focused mainly to exchange electrons between a conductive substrate

and a redox couple either in the solution or chemically attached to the CNTs. The ability for CNTs to function as nanowires was elegantly demonstrated by Gooding's (Gooding *et al.*, 2003) group, where electron communication was observed between the underlying electrode and electroactive proteins chemically bound on CNTs. Wong (Wong *et al.*, 2008) reported the use of carbon nanotubes (CNTs) as nanoreaction vessels to confine chemical reactions within the carbon nanotestube. This was achieved by functionalizing two redox reagents, anthraquinonnyl and 4-nitrophenyl groups, on the same CNT. To the best of our knowledge, this is the first reported case of dual-molecule functionalization of CNTs and illustration of the occurrence of a chemical reaction at the CNT surface. In the experimental section, the CNTs, which are commercially available bamboo-type MWCNTs with the length of 5 – 20 µm and outer diameter of 30 µm, were dually functionalized using the aryl diazonium chemistry. Both AQ and NP were chemically functionalized on the same CNTs by using a similar diazonium-CNT derivatization protocol, forming AQ-NP-MWCNTs. The cyclic voltammogram scan of AQ-NP-MWCNTs was investigated referring to oxidation and reduction peaks of the system. A redox reaction mechanism was proposed where $AQH_2$ is the oxidizing agent with the oxidation peak at $E_a$ = –0.385 V while $NHOH–C_6H_4$ is the reducing group gradually lessening the peak currents of the oxidation peak at $E_a$ = 0.125 V. In addition, it was found that the CNT can mediate the chemical reaction between the two redox reagents and generate 4-arylamine groups at the CNT surface. The reaction can proceed only when both the reagents are confined on the same CNT; if the reagents are located on different tubes, reaction ceases. The exact mechanism of electron transfer from $AQH_2$ to the 4-arylhydroxyl amine group, whether it occurs by electron tunneling between reagents or by hopping in the CNT was unknown at that time. However, the fact that the reaction proceeds to completion suggests the latter because statistically path that the reagents need to pass must be further apart that the electron distance for tunneling.

Because CNT is a low dimensional nanomaterial that elongates in only one dimension, computational studies of the CNT should investigate elaborately in the length of elongation. An example of the CNT studies was reported by Wu (Wu *et al.*,

2008) on the topic of carbon nanobuds carried out using the linear combination of atomic orbital density functional theory (DFT) method implemented in the DMol3 package. This periodic calculation was performed in order to overcome the length limitation of CNT models. Although only Γ point was considered in the Brilliouin zone for the geometric optimization, *k* point was extended to be 1 × 1 × 10 for investigating the electronic properties. In addition, an intermolecular interaction between two neighboring carbon nanotubes or between two adjacent active/functionalized groups can produce a significant error of the calculation. To overcome this problem, the nearest distance between the two SWCNTs was set to be greater than 25 Å, and that between two functionalized groups (fullerenes) is greater than 13 Å.

After the discovery of multi-walled carbon nanotubes by Iijima in 1991 (Iijima, 1991), single-walled carbon nanotubes were produced in 1993 by Iijima (Iijima *et al.*, 1993) and Bethune (Bethune *et al.*, 1993) with more details of tubule helicity following Hamada's notation. The single-shell tubules were proposed that they might be the embryo for the multi-shell tubules. In the proposed model for the nanotube growth, the tubule ends were open so that carbon atoms were easily captured at dangling bonds, and the multi-shell tubules grew in the direction of the tube axis and also perpendicular to it. The structure of a SWCNT can be conceptualized by wrapping a one-atom-thick layer of graphite called graphene into a seamless cylinder. The way the graphene sheet was wrapped was represented by a pair of indices (*n*,*m*) called the chiral vector. Lu described the geometry, helicity, electronic structures, and aromaticity of SWCNTs in 2005 (Lu *et al.*, 2005). The integers *n* and *m* denote the number of unit vectors along two directions in the honeycomb crystal lattice of grapheme. If *m* = 0, the nanotubes are called zigzag. If *n* = *m*, the nanotubes are called armchair. Otherwise, they are called chiral. Because of the symmetry and unique electronic structure of grapheme, the structure of a nanotube strongly affects its electrical properties. For a given (*n*,*m*) nanotube, if *n* – *m* is a multiple of 3, then the nanotube is metallic with none band gap or with a very small band gap (in range 0.00 to 0.50 eV), otherwise the nanotube is a moderate

semiconductor. Thus all armchair ($n = m$) nanotubes including nanotubes with $n - m = 3i$ ($i$ = integer), i.e. (6,0), (9,0), (7,1), etc., are metallic, and other nanotubes (6,5), (9,2), etc. are semiconducting.

# METHODS OF CALCULATIONS

The periodic calculations were carried out using the density functional theory (DFT) method as implemented in the DMol3 package (Delley, 1990; Delley, 2000). For all functionals that we investigated, the generalized gradient approximation (GGA) and an all-electron double numerical basis set with polarized function (DNP) were chosen for these spin-unrestricted computations. These functionals can be applied to large periodic systems and were known to bring about reliable qualitative results. The density functionals used in this work did not include dispersion energy contributions. The DNP basis set corresponds to a double-ζ quality basis set with a p-type polarization function added to hydrogen and d-type polarization functions added to heavier atoms, and is comparable to 6-31G** Gaussian basis sets, providing a better accuracy, particularly for the hydrogen removal step. The real space global cutoff radius was set to be 3.70 Å. For the geometrical optimizations, all atoms were fully optimized until all the forces on the atoms were less than 0.05 eV $Å^{-1}$. The Brillouin zone was sampled using the Monkhorst-Pack scheme (Monkhorst *et al.*, 1976).

## 1. Calibration of the SWCNTs

In the present approach, a suitably calibrated SWCNT was used to mimic the multi-walled tubes used in the experiments for the computations. The important feature was that the MWCNTs used in the experiments had electronic band gaps like semiconductors. The criterion for the calibration was thus, that the gap of the model-tube should be in the range of 0.5 to 1.5 eV (O'Connell *et al.*, 2002). The calibration was started with a study of naked (*n*,0) zigzag SWCNTs, investigated with three functionals and comparing the energy gaps (*E*gap) with each other and with the ones obtained in previous studies. Each initial structure was generated in a supercell periodic box of 20 × 20 × 8.52 $Å^3$, composed of two repeated unit cells of SWCNT along the tube axis. The closest distance between two neighboring SWCNTs was larger than 10 Å in order to be able to ignore intertube interactions in the calculations.

**Table 1** Energy gap (eV) of pristine (*n*,0) SWCNTs calculated with the BLYP, PBE, and PW91 methods and DNP basis set. Average deviation of energy gap (eV) investigated relatively with the previous theoretical data.

| SWCNT | Energy gap / eV | | | | | | | |
|---|---|---|---|---|---|---|---|---|
| | BLYP | PBE | PW91 | Reference data | | | | |
| | | | | *calc* | *expt* | *calc* | *calc* | *calc* |
| (6,0) | 0.00 | 0.00 | 0.00 | 0.00 | – | – | – | – |
| (7,0) | 0.11 | 0.15 | 0.16 | – | – | – | 0.21 | 0.19 |
| (8,0) | 0.66 | 0.62 | 0.61 | 0.643 | – | 0.62 | – | 0.59 |
| (9,0) | 0.24 | 0.17 | 0.17 | – | 0.080 | 0.17 | – | – |
| (10,0) | 0.61 | 0.68 | 0.69 | – | – | – | – | – |
| (11,0) | 1.00 | 0.97 | 0.97 | – | – | – | – | – |
| (12,0) | 0.19 | 0.14 | 0.14 | 0.078 | 0.042 | – | – | – |
| Average deviation | ±0.079 | ±0.044 | | | | | | |

The calibrations were performed in the GGA in the Perdew-Burke-Ernzerhof (PBE) (Perdew *et al.*, 1996), Becke's exchange and Lee, Yang, and Parr's correlation functional (BLYP) (Becke, 1988; Lee *et al.*, 1988), and non-local exchange-correlation functional (PW91) (Perdew *et al.*, 1992) with the maximum *k* points of 1 × 1 × 50. These calculated energy gaps and reference data show in Table 1 with average deviation values of each method. The BLYP method was immediately disqualified due to its large average deviation of ±0.079 eV in *E*gap compared to previous theoretical data (Blase *et al.*, 1994; Ouyang *et al.*, 2001; Gülseren *et al.*, 2002; Zólyomi *et al.*, 2004; Valavala *et al.*, 2008; Pannopard *et al.*, 2009). The PBE and PW91 methods gave the same *E*gap within a small deviation of ±0.007 eV and a smaller deviation of ±0.044 eV compared to the same data. Although these two methods were very similar, the PBE functional was chosen in our calculations,

following the recent theoretical studies (Wu *et al.*, 2008; Zhao *et al.*, 2008) of periodic systems.

The diameter of the zigzag SWNCTs was then varied systematically and the band gaps studied with the same procedure to find the smallest nanotube representative of the experimental system. Three (*n*,0) SWCNTs with *n* mod 3 = 0 were found to be metallic, obeying the empirical (*n*,*n* + 3*i*) rule for metallic carbon nanotubes, also known as the 1/3 rule: (6,0) with an *E*gap of 0.00 eV (Ref. *E*gap,*calc*= 0.00 eV (Gülseren *et al.*, 2002)); (9,0) with an *E*gap of 0.17 eV (Ref. *E*gap,*expt* = 0.080 ±0.005 (Ouyang *et al.*, 2001), and *E*gap,*calc* = 0.17 (Blase *et al.*, 1994) eV); and (12,0) with an *E*gap of 0.14 eV (Ref. *E*gap,*expt* = 0.042 ±0.004 (Ouyang *et al.*, 2001) and *E*gap,*calc* = 0.078 (Gülseren *et al.*, 2002) eV), (where *expt* is experimental data, *calc* is theoretical data, and *i* is an integer). The (7,0) SWCNT also presented a metallic character with an 0.15 eV energy gap (Ref. 0.21 (Zólyomi *et al.*, 2004), 0.19 (Valavala *et al.*, 2008) eV). Thus, the (6,0), (7,0), (9,0), and (12,0) SWCNTs were certainly not usable as models because of their metallic character.

The (8,0) SWCNT was found to be the smallest zigzag carbon nanotube that displayed a semiconducting behavior with an acceptable energy gap of 0.62 eV. The calculated value was in good agreement with previous data for the *E*gap (0.643 (Gülseren *et al.*, 2002), 0.62 (Blase *et al.*, 1994), 0.59 (Valavala *et al.*, 2008), 0.63 (Pannopard *et al.*, 2009) eV) and confirmed that the *E*gap of *n* mod 3 = 2 tubes was larger than that *n* mod 3 = 1 (Valavala *et al.*, 2008). In order to be able to neglect the intermolecular interaction between the two redox species, the six repeated unit cells along the z-direction of the carbon nanotube were used for the calculations of functionalized tubes. Therefore, the SWCNT-mediated redox models in this work were generated from the validated (8,0) SWCNT and calculated by periodic calculations with the PBE method.

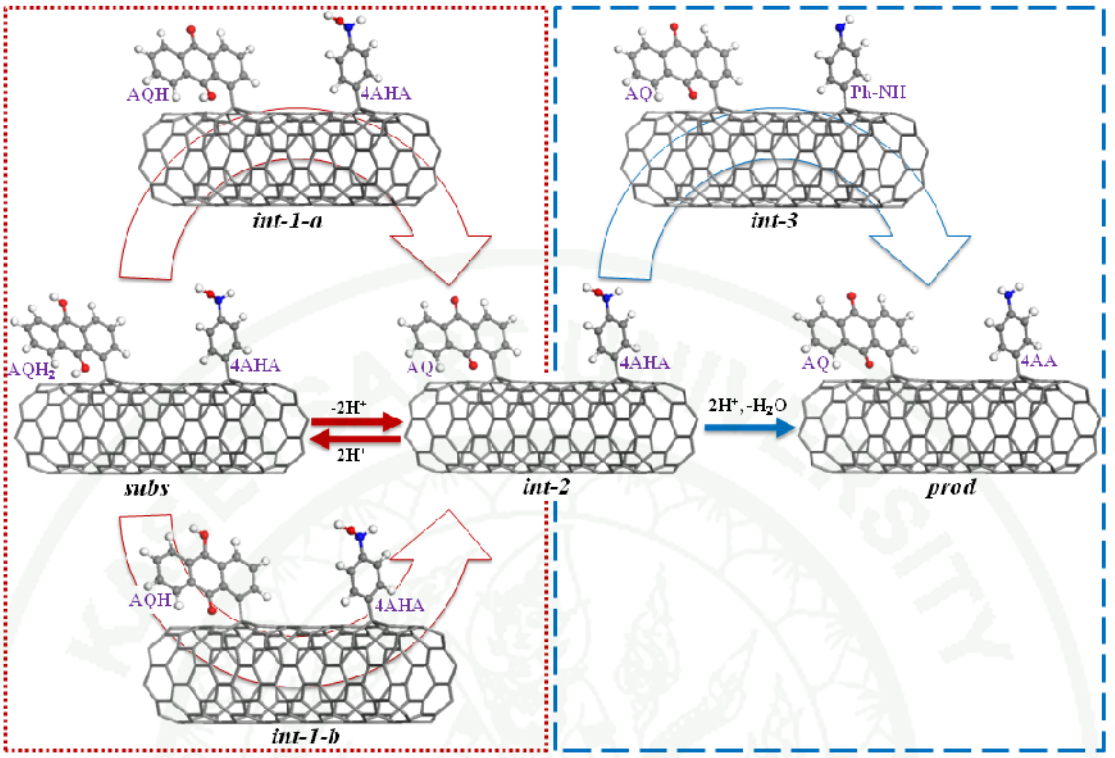

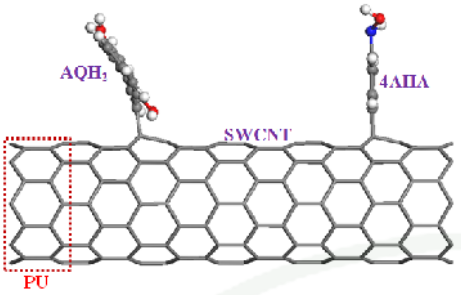


(a)

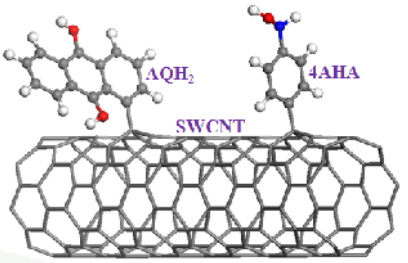


(c)

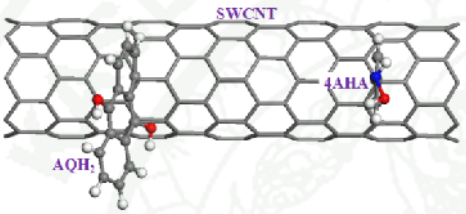


(b)

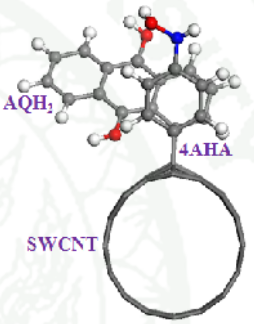


(d)

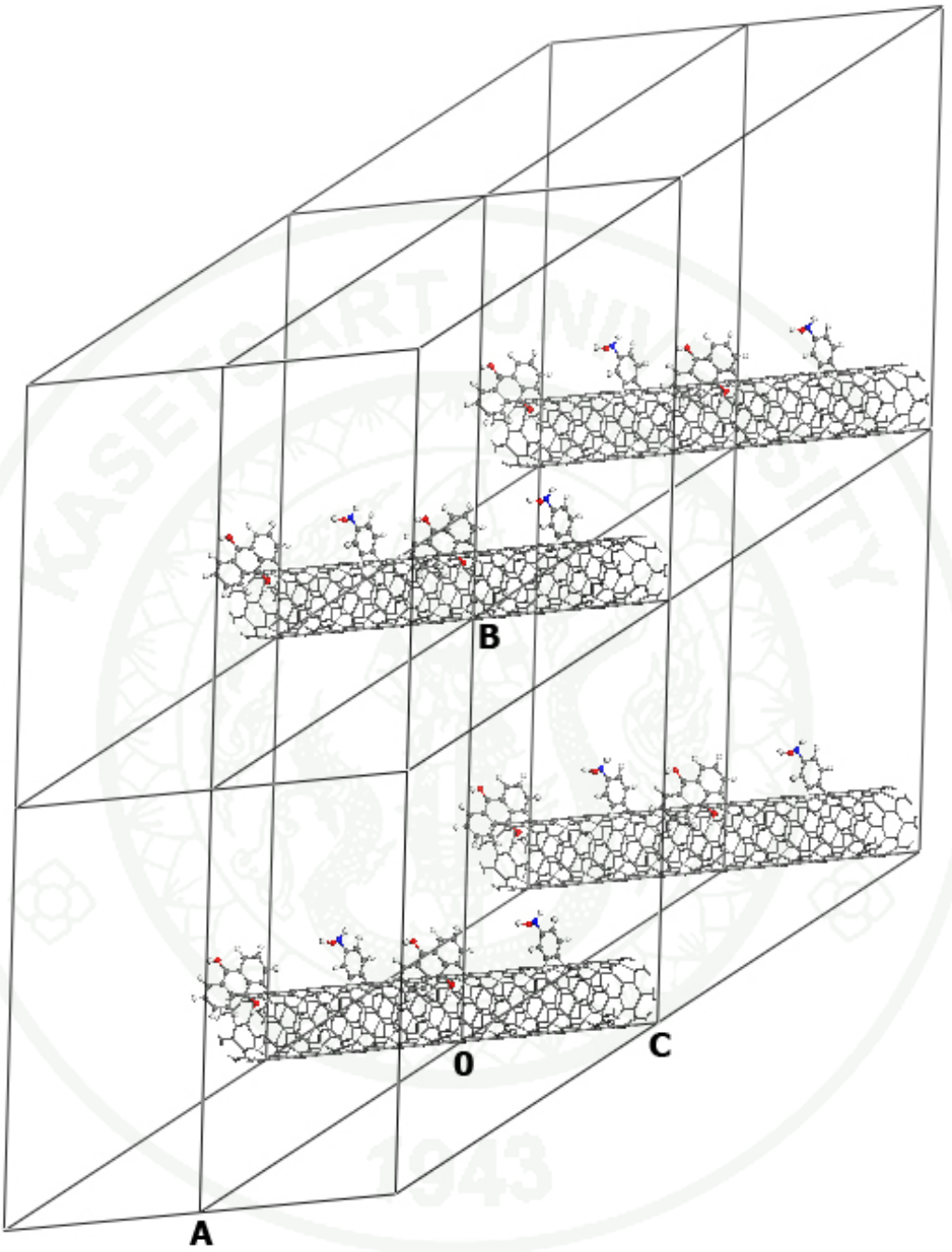

## 2. Redox systems

As seen above, an (8,0) SWCNT was chosen. For the full redox system, it was functionalized by two redox groups more than 12 Å apart from each other to minimize, and eventually neglected, the intermolecular interaction between these two species. A supercell with $40 \times 40 \times 24.15$ $Å^3$, comprising six periodic lengths for the zigzag SWCNT, was adopted in the calculation with the PBE function (see Figure 3(a)). Each supercell contained two redox groups, which were covalently bonded to the sidewall of the SWCNT. The smallest distance between two neighboring SWCNTs was larger than 30 Å. In order to save computational time, the *k* points were reduced to be $1 \times 1 \times 10$, following the previous study (Wu *et al.*, 2008), to calculate the electronic properties of the full redox system. Only the Γ point in the Brillouin zone was also considered for the geometric optimization and orbital analysis.

Even though the individual processes in the overall redox reaction take place concurrently, we simplified the problem by dividing the full redox pathway into six hypothetical states (see Figure 2), which are: $AQH_2$-SWCNT-4AHA (substrate: *subs*), $[AQH\text{-}SWCNT\text{-}4AHA]^{1-}$ (intermediate-1), $[AQ\text{-}SWCNT\text{-}4AHA]^{2-}$ (intermediate-2: *int-2*), $[AQ\text{-}SWCNT\text{-}Ph\text{-}NH]^{1-}$ (intermediate-3: *int-3*) and AQ-SWCNT-4AA (product: *prod*) ($AQH_2$ = anthraquinolyl, AQ = anthraquinonyl, 4AHA = 4-arylhydroxyl amine, 4AA = 4-arylamine, SWCNT = (8,0) zigzag SWCNT). The intermediate-1 state can be considered in two configurations, which are termed intermediate-1-a (*int-1-a*) and intermediate-1-b (*int-1-b*) for the removal of H*a* and H*b*, respectively.

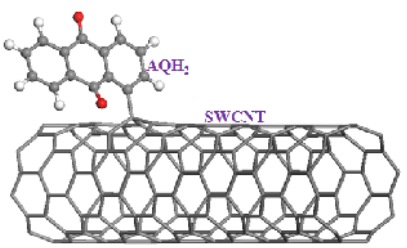


(a)

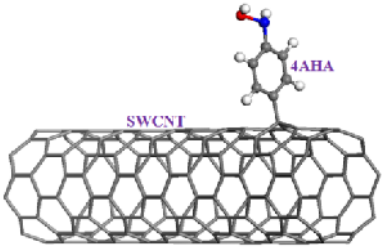


(b)

# RESULTS AND DISCUSSION

The diazonium method provided a well-defined chemical bond between the molecule and a carbon atom of the tube rather than the less well defined interaction between an entire group and the tube surface found in the adsorption of π-conjugated molecules. Indeed, the optimized geometry of the functionalized SWCNTs in the full redox system shown that the reacting groups with closing carbon atoms of the nanotube changed their geometries with an average displacement of 0.19 Å for the AQ derivatives and 0.22 Å for the 4AHA derivatives. While the remaining atoms, which are far from the reacting species, of the tube remained roughly at the same positions within, on an average, 0.06 Å. These averages were calculated for all atoms of a desired part changing their relative positions in each step of the mechanism. We also found that the phenyl plane of the 4AHA group (including its derivatives: Ph-NH, and 4AA) was parallel to the perpendicular axis (reference line), which was vertical to the tube axis of the SWCNT medium, as shown in Figures 6. The angle between the anthraquinonyl plane of the $AQH_2$ group in *subs* and the reference line was sharp, about 30 degrees, due to the steric effect to the adjacent hydrogen atom (H*b*) of the hydroxyl moiety of the $AQH_2$ group (see Figure 3(a)). Whenever this hydrogen atom was cleaved, the repulsive force on the ketone became smaller. Thus, a less sharp angle was found, about 10 degrees. However, the AQ group was not exactly sharp to the reference line, because the carbonyl oxygen atom was a hindrance for such an orientation.

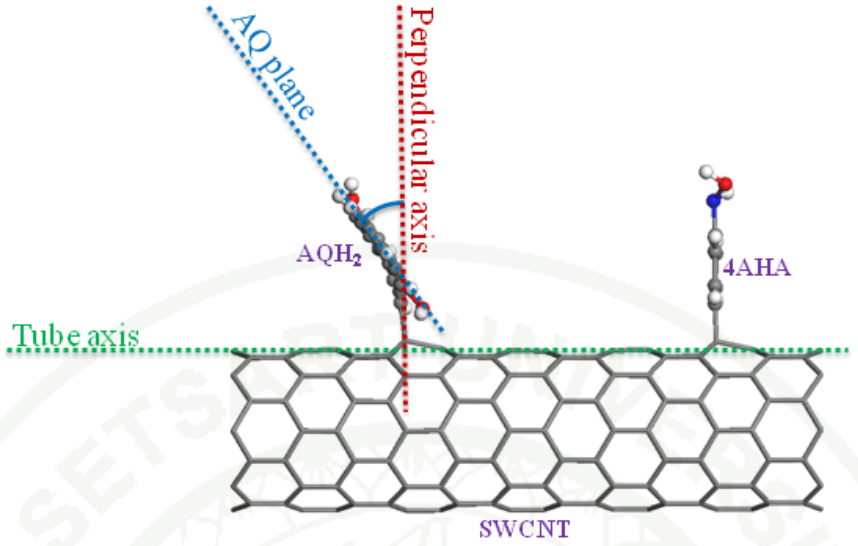

**Table 2** Hirshfeld partial charge (in elementary changes *e*), energy gap (eV), and relative energy (kcal $mol^{-1}$) calculated with the PBE method and DNP basis set for pristine SWCNT, substrate, intermediate, product, and single functionalized systems. (D = direct, I = indirect energy gap)

| Entry | Structure | Hirshfeld charge | | | | Egap / eV | Erel / kcal $mol^{-1}$ |
|---|---|---|---|---|---|---|---|
| | | Partial charge | | | Total | | |
| 1 | Pristine SWCNT | - | - | - | - | 0.62 D | - |
| 2 | Substrate | $AQH_2$ = 0.05 | SWCNT = -0.07 | 4AHA = 0.03 | 0.01 | 0.00 | - |
| 3 | Intermediate-1-a | AQH = -0.06 | SWCNT = -0.91 | 4AHA = -0.02 | -0.99 | 0.04 D | 0.00 |
| 4 | Intermediate-1-b | AQH = -0.16 | SWCNT = -0.81 | 4AHA = -0.02 | -0.99 | 0.04 I | -0.95 |
| 5 | Intermediate-2 | AQ = -0.19 | SWCNT = -1.73 | 4AHA = -0.07 | -1.99 | 0.10 I | - |
| 6 | Intermediate-3 | AQ = -0.07 | SWCNT = -0.77 | Ph-NH = -0.16 | -1.00 | 0.16 I | - |
| 7 | Product | AQ = -0.01 | SWCNT = -0.03 | 4AA = 0.05 | 0.01 | 0.00 | - |
| 8 | $[AQ\text{-}SWCNT]^{2-}$ | AQ = -0.27 | SWCNT = -1.72 | - | -1.99 | 0.00 | - |
| 9 | $[4AHA\text{-}SWCNT]^{2-}$ | - | SWCNT = -1.92 | 4AHA = -0.07 | -1.99 | 0.00 | - |

The electronic properties of the redox systems were reported in Table 1. The results show that the two configurations of intermediate-1 had relative energy which differed by –0.95 kcal $mol^{-1}$, the *int-1-b* being more favorable than *int-1-a* due to a smaller steric effect between the hydrogen atom of the AQH group (H*b*) and the nanotube. The proposed mechanism pathway of the redox reaction through *int-2* was presented in snapshots. It started from the *subs* configuration and went through *int-1-b*, *int-2*, and *int-3* to *prod*. In more detail: The O-H*b* of the *subs* was first cleaved, as demonstrated in the *int-1-b*, with one electron remaining. Sequentially, the O-H*a* was removed, resulting in the *int-2*. This was a half-cell redox reaction, with, overall, two electrons left. The *int-3* was an intermediate state, corresponding to the *int-2* to *prod* reduction, where a hydroxyl group of the 4AHA was dehydrated by an acidic proton addition, and the Ph-NH group remained. The nucleophilic nitrogen atom of the *int-3* was then also attacked by another electrophilic proton, resulting in the *prod* configuration. The reduction reaction cannot be reversible: A negative –0.26 *e* local Hirshfeld charge was found on the nucleophilic nitrogen atom of the Ph-NH part of *int-3*. This made an attack between this site and an oxygen atom of water highly unlikely.

The chemical attachment of the two redox reagents to the SWCNT created new impurity states within the band gap. From the pristine SWCNT, *E*gap = 0.62 eV, the band gap in the redox systems was lowered to less than 0.16 eV, thereby introducing a more metallic character to the system. This eased electron delocalization in the modified system. The electron density difference and Hirshfeld partial charges analyses show that the tube can hold 87% of the extra electron density of the hypothetical negative intermediate produced from the oxidation of the $AQH_2$ (see Entry 5 in Table 1). In addition, the remaining charge at the AQ in the *int-2* was –0.19 *e*, leading to a reverse reduction of the AQ to the $AQH_2$.

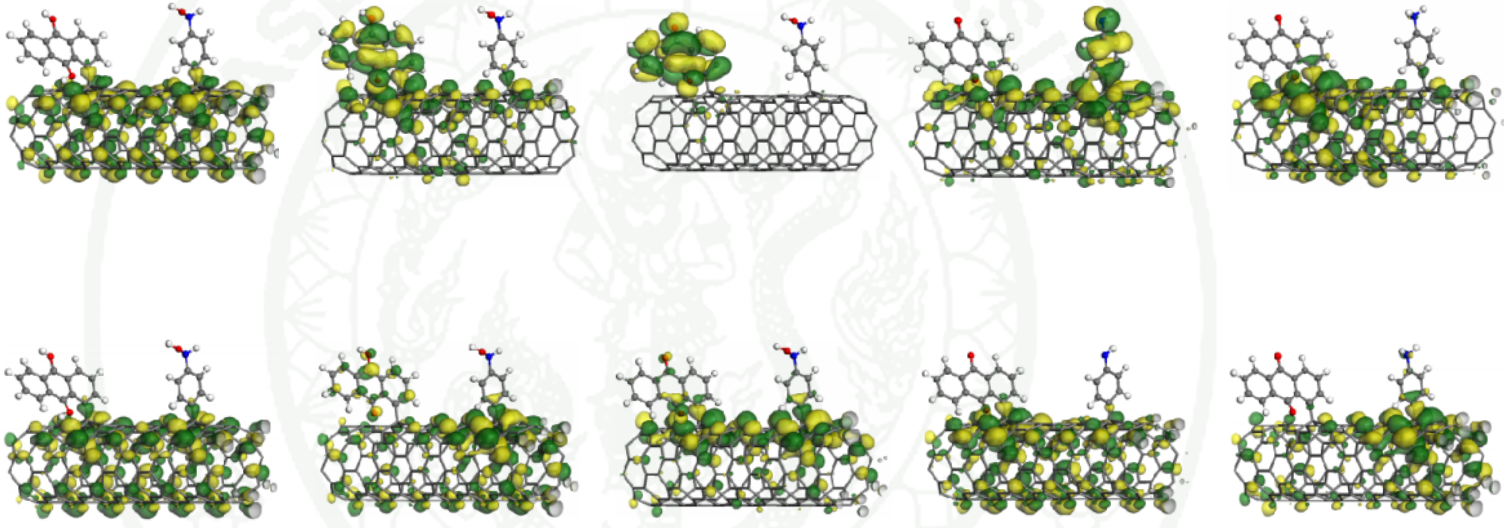

(a) (b) (c) (d) (e)

**Figure 7** LUMO (top) and HOMO (bottom) of *subs* (a), *int-1-b* (b), *int-2* (c), *int-3* (d), and *prod* (e) were plotted for an isovalue of ±0.015 *e* $Å^{-3}$.

The frontier molecular orbitals of the redox system were illustrated in Figure 7. An electron ionization and reception occurred at the SWCNT, which can be clearly observed at both the HOMO and LUMO for the substrate. In the intermediate steps, an electronic connection between the AQ and the 4AHA molecules was clearly shown at the HOMO level. An electron movement was proposed as a theoretical mechanism pathway. The first electron from the oxidation reaction of the $AQH_2$ to AQH was initially excited to occupy the LUMO level of the *int-1-b*. In this state, both the AQ group and the nanotube were occupied, as shown in the LUMO level in Figure 7(b). After that, the second electron was generated from the oxidation of the AQH to AQ, resulting in two excited electrons occupying strongly only in the AQ part in the LUMO level of the *int-2*. This case confirmed the reversible reaction of the AQ to $AQH_2$. These two electrons then transferred to the 4AHA part, resulting in the strong occupation in the 4AHA side (Ph-NH) as shown in the LUMO level in Figure 7(d). The Ph-NH group was eventually reduced by the extra electron at that level, resulting in the 4AA. The HOMO of the *prod* shown that the electrons were distributed mostly at the 4AA and no longer occupied the AQ side. In addition, an electron in the *int-1-b* and *int-2*, which was strongly localized at the AQ part, confirmed that it can reversely reduce. This is the reduction reaction from AQ to $AQH_2$. On the other hand, an electron was rarely available at the 4AHA group (Ph-NH) in the *int-2* and *int-3*, leading to an irreversible reduction.

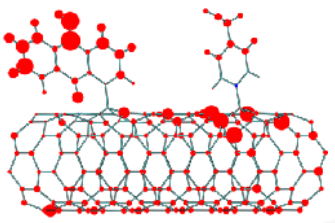

(a)-1

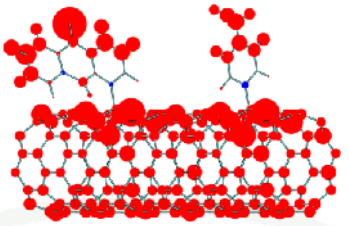

(a)-2

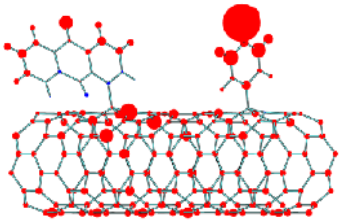

(a)-3

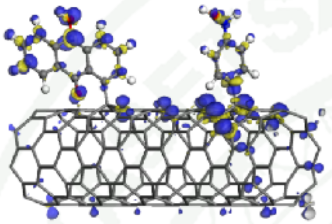

(b)-1

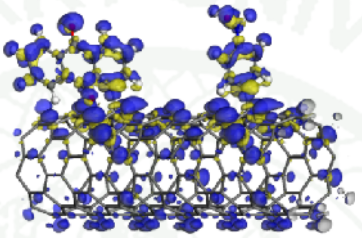

(b)-2

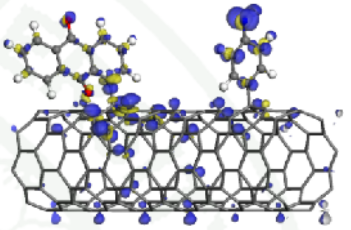

(b)-3

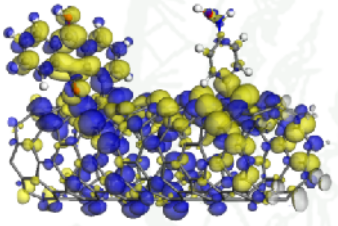

(c)-1

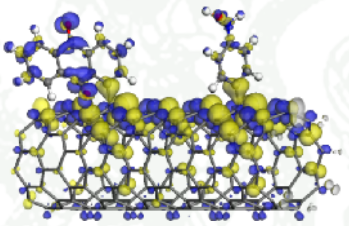

(c)-2

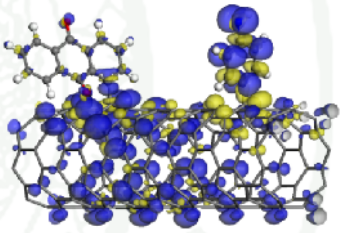

(c)-3

The plots of the difference of the Hirshfeld charge were presented in Figures 8(a). These plots were calculated from the difference of each atomic charge between the negatively-charged structure and its neutralized version, neglecting relaxations, resulting in the charge difference of the negative atomic charge. An electron in the intermediate states had a high probability of presence at the AQH, leading to the reverse reduction of AQH to $AQH_2$. Two electrons in the *int-2* step had high probabilities at the AQ, 4AHA, and at the bridge in the nanotube, as shown in Figure 8(a)-2. Therefore, it was clearly verified that the AQ and 4AHA groups can be reduced to $AQH_2$ and 4AA, respectively.

Figure 8(b) shows the calculated disparity of the electron densities, following the definition; $\Delta\rho(\mathbf{i}\rightarrow\mathbf{j}) = \rho(\mathbf{j}) - \rho(\mathbf{i})$, where $\Delta\rho(\mathbf{i}\rightarrow\mathbf{j})$ is the change of negative charge densities between the negatively-charged structure, $\rho(\mathbf{j})$, and its neutralized version, $\rho(\mathbf{i})$, resulting in the density of only the negative charge. This plot clearly shows the connection between the reducing group and the oxidizing group. The electron density obviously occupied only the redox molecules and their junction to the SWCNT medium.

The nucleophilic Fukui function plots, as demonstrated in Figure 8(c), confirmed the electron hopping process of the redox reaction via the nanotube. The mechanism started with a high nucleophilic character of the AQ and its connection. Then, the reducing negative behavior at the AQ led to an increase at 4AHA. However, the two carbon atoms of the nanotube connected to the AQ and 4AHA species are of the non-conjugated $sp^3$ type. The negative charge density was high at the bridging single bonds of both of the carbon atoms, as depicted in Figures 8(c)-1 to 8(c)-3, opening a route for the electron transfer from the reducing AQ group to the other. Therefore, the electron transfer between two redox groups can occur by electron hopping via the SWCNT.

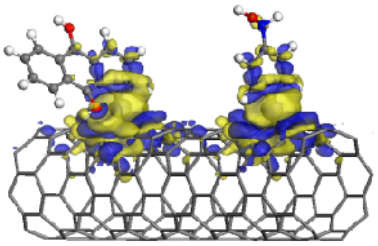

(a)

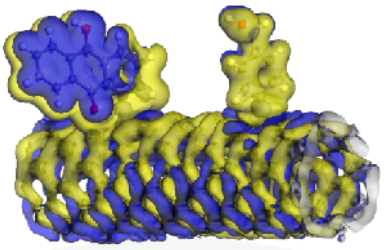

(b)

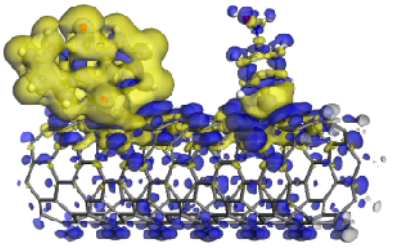

(c)

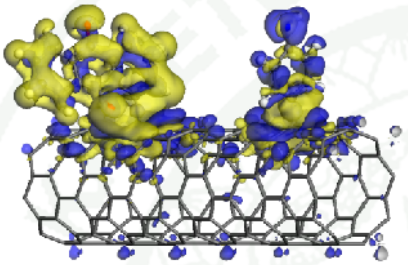

(d)

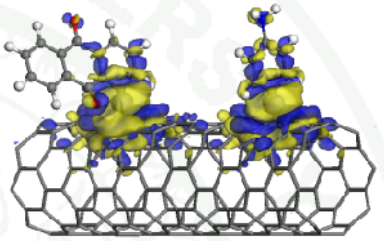

(e)

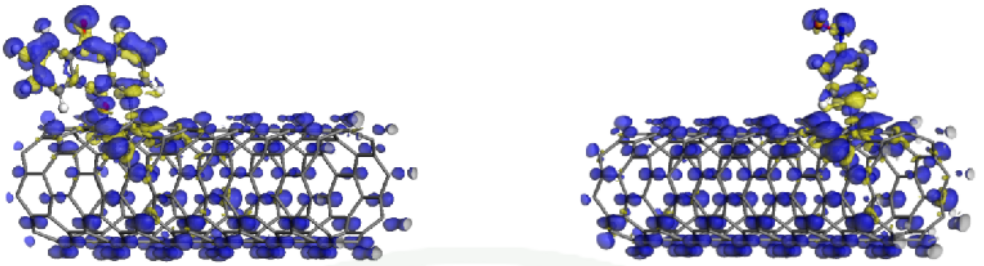

(a) (b)

# CONCLUSIONS

DFT calculations with the PBE functional were used to investigate the reaction mechanism of electron hopping in the SWCNT-mediated redox reaction of anthraquinonyl ($AQH_2$-) and 4-arylhydroxyl amine (4AHA-) groups. Our findings can be summarized into three main points. First, the disparity of electron densities, partial electron density difference, and Hirshfeld partial charges analysis show that the SWCNT can hold 87% of the extra electron density of the hypothetical negative intermediate produced from the oxidation of $AQH_2$. Second, the chemical attachment of these two redox reagents to the SWCNT also caused new impurity states to appear within the band gap, thereby introducing a more metallic character to the system. Third, the electrons from the oxidized $AQH_2$ group can be transferred to the oxidizing 4AHA group at the other end of the nanotube by a hopping process through the mediating SWCNT. This mechanism was confirmed by the non-localized distribution of the hopping excited electrons. These findings provided a detailed understanding of the electron hopping process and agreed well with previous experimental study. This work was not only complementing experimental study by giving an interpretation in terms of electronic wave functions, but also demonstrated a promising application of the CNT materials in the nanotechnology field.

# LITERATURE CITED

Baughman, R.H., A.A. Zakhidov and W.A. de Heer. 2002. Carbon Nanotubes--the Route Toward Applications. **Science** 297(5582): 787-792.

Becke, A.D. 1988. Density-functional exchange-energy approximation with correct asymptotic behavior. **Physical Review A** 38(6): 3098.

Bethune, D.S., C.H. Klang, M.S. de Vries, G. Gorman, R. Savoy, J. Vazquez and R. Beyers. 1993. Cobalt-catalysed growth of carbon nanotubes with single-atomic-layer walls. **Nature** 363(6430): 605-607.

Blase, X., L.X. Benedict, E.L. Shirley and S.G. Louie. 1994. Hybridization effects and metallicity in small radius carbon nanotubes. **Physical Review Letters** 72(12): 1878-1881.

Charles G. R. Heald, G.G.W., Li Jiang, Timothy G. J. Jones, Richard G. Compton,. 2004. Chemical Derivatisation of Multiwalled Carbon Nanotubes Using Diazonium Salts13. **ChemPhysChem** 5(11): 1794-1799.

de Heer, W.A., A. Châtelain and D. Ugarte. 1995. A Carbon Nanotube Field-Emission Electron Source. **Science** 270(5239): 1179-1180.

Delley, B. 1990. An all-electron numerical method for solving the local density functional for polyatomic molecules. **The Journal of Chemical Physics** 92(1): 508-517.

Delley, B. 2000. From molecules to solids with the DMol[sup 3] approach. **The Journal of Chemical Physics** 113(18): 7756-7764.

Gooding, J.J., R. Wibowo, J.Q. Liu, W. Yang, D. Losic, S. Orbons, F.J. Mearns, J.G. Shapter and D.B. Hibbert. 2003. Protein Electrochemistry Using Aligned Carbon Nanotube Arrays. **J. Am. Chem. Soc.** 125(30): 9006-9007.

Gülseren, O., T. Yildirim and S. Ciraci. 2002. Systematic ab initio study of curvature effects in carbon nanotubes. **Physical Review B - Condensed Matter and Materials Physics** 65(15): 1534051-1534054.

Iijima, S. 1991. Helical microtubules of graphitic carbon. **Nature** 354(6348): 56-58.

Iijima, S. and T. Ichihashi. 1993. Single-shell carbon nanotubes of 1-nm diameter. **Nature** 363(6430): 603-605.

Kong, J., N.R. Franklin, C. Zhou, M.G. Chapline, S. Peng, K. Cho and H. Dai. 2000. Nanotube Molecular Wires as Chemical Sensors. **Science** 287(5453): 622-625.

Lee, C., W. Yang and R.G. Parr. 1988. Development of the Colle-Salvetti correlation-energy formula into a functional of the electron density. **Physical Review B** 37(2): 785.

Leventis, H.C., I. Streeter, G.G. Wildgoose, N.S. Lawrence, L. Jiang, T.G.J. Jones and R.G. Compton. 2004. Derivatised carbon powder electrodes: Reagentless pH sensors. **Talanta** 63(4): 1039-1051.

Lu, X. and Z. Chen. 2005. Curved Pi-Conjugation, Aromaticity, and the Related Chemistry of Small Fullerenes (<C60) and Single-Walled Carbon Nanotubes. **Chemical Reviews** 105(10): 3643-3696.

Monkhorst, H.J. and J.D. Pack. 1976. Special points for Brillouin-zone integrations. **Physical Review B** 13(12): 5188.

O'Connell, M.J., S.M. Bachilo, C.B. Huffman, V.C. Moore, M.S. Strano, E.H. Haroz, K.L. Rialon, P.J. Boul, W.H. Noon, C. Kittrell, J. Ma, R.H. Hauge, R.B. Weisman and R.E. Smalley. 2002. Band Gap Fluorescence from Individual Single-Walled Carbon Nanotubes. **Science** 297(5581): 593-596.

Ouyang, M., J.-L. Huang, C.L. Cheung and C.M. Lieber. 2001. Energy Gaps in "Metallic" Single-Walled Carbon Nanotubes. **Science** 292(5517): 702-705.

Pandurangappa, M., N.S. Lawrence and R.G. Compton. 2002. Homogeneous chemical derivatisation of carbon particles: A novel method for funtionalising carbon surfaces. **Analyst** 127(12): 1568-1571.

Pannopard, P., P. Khongpracha, M. Probst and J. Limtrakul. 2009. Gas sensing properties of platinum derivatives of single-walled carbon nanotubes: A DFT analysis. **Journal of Molecular Graphics and Modelling** 28(1): 62-69.

Patolsky, F., Y. Weizmann and I. Willner. 2004. Long-range electrical contacting of redox enzymes by SWCNT connectors. **Angewandte Chemie-International Edition** 43(16): 2113-2117.

Perdew, J.P., K. Burke and M. Ernzerhof. 1996. Generalized Gradient Approximation Made Simple. **Physical Review Letters** 77(18): 3865.

Perdew, J.P. and Y. Wang. 1992. Accurate and simple analytic representation of the electron-gas correlation energy. **Physical Review B** 45(23): 13244.

Tans, S.J., A.R.M. Verschueren and C. Dekker. 1998. Room-temperature transistor based on a single carbon nanotube. **Nature** 393(6680): 49-52.

Valavala, P.K., D. Banyai, M. Seel and R. Pati. 2008. Self-consistent calculations of strain-induced band gap changes in semiconducting (n,0) carbon nanotubes. **Physical Review B - Condensed Matter and Materials Physics** 78(23).

Wildgoose, G.G., M. Pandurangappa, N.S. Lawrence, L. Jiang, T.G.J. Jones and R.G. Compton. 2003. Anthraquinone-derivatised carbon powder: Reagentless voltammetric pH electrodes. **Talanta** 60(5): 887-893.

Wong, E.L.S. and R.G. Compton. 2008. Chemical reaction of reagents covalently confined to a nanotube surface: Nanotube-mediated redox chemistry. **Journal of Physical Chemistry C** 112(22): 8122-8126.

Wu, X. and X.C. Zeng. 2008. First-Principles Study of a Carbon Nanobud. **ACS Nano** 2(7): 1459-1465.

Zhao, J.-x. and Y.-h. Ding. 2008. Chemical Functionalization of Single-Walled Carbon Nanotubes (SWNTs) by Aryl Groups: A Density Functional Theory Study. **The Journal of Physical Chemistry C** 112(34): 13141-13149.

Zólyomi, V. and J. Kürti. 2004. First-principles calculations for the electronic band structures of small diameter single-wall carbon nanotubes. **Physical Review B - Condensed Matter and Materials Physics** 70(8).

# APPENDIX

## PRESENTATIONS AND PUBLICATION:

- **Electron hopping process in SWCNT-mediated redox reaction: an evidence observed by DFT theory**

**Teeranan Nongnual**, Saowapak Choomwattana, Somkiat Nokbin, Pipat Khongpracha and Jumras Limtrakul. Abstract of paper Congress on The 2009 NSTI Nanotechnology Conference and Trade Show, Houston, United States of America, May 1-8, 2009. (Poster Presentation)

- **Density functional theory evidence for an electron hopping process in single-walled carbon nanotube-mediated redox reactions**

**Teeranan Nongnual**, Somkiat Nokbin, Pipat Khongpracha, Philippe Anthony Bopp, and Jumras Limtrakul 2010. " Density functional theory evidence for an electron hopping process in single-walled carbon nanotube-mediated redox reactions." Carbon **48**(5): 1524-1530.

- **Density functional theory evidence for an electron hopping process in single-walled carbon nanotube-mediated redox reactions**

**Teeranan Nongnual**, Somkiat Nokbin, Pipat Khongpracha, Philippe Anthony Bopp, and Jumras Limtrakul. Abstract of paper Congress on The 1st National Research Symposium on Petroleum, Petrochemicals, and Advanced Materials and The 16th PPC Symposium on Petroleum, Petrochemicals, and Polymers, Bangkok, Thailand, April 22, 2010. (Oral Presentation)

# CURRICULUM VITAE

**NAME** : Mr. Teeranan Nongnual

**BIRTH DATE** : December 21, 1985

**BIRTH PLACE** : Nakhon Si Thammarat, Thailand

**NATIONALITY** : Thai

**EDUCATION**

| | **YEAR** | **INSTITUTION** | **DEGREE** |
|---|---|---|---|
| : | 2003 | Prince of Songkla University | B.Sc. (Chemistry) |

**SCHOLARSHIPS** : Scholarship from the Development and Promotion of Science and Technology Talents Project (DPST) 2000-2010

: Scholarship from the Postgraduate on Education and research in Petroleum and Petrochemical Technology (ADB-MUA) 2007-2010

CARBON 48 (2010) 1524–1530

available at www.sciencedirect.com

ScienceDirect

journal homepage: www.elsevier.com/locate/carbon

# Density functional theory evidence for an electron hopping process in single-walled carbon nanotube-mediated redox reactions

*Teeranan Nongnual* [a,b], *Somkiat Nokbin* [a,b], *Pipat Khongpracha* [a,b], *Philippe Anthony Bopp* [c], *Jumras Limtrakul* [a,b,*]

[a] *Laboratory for Computational and Applied Chemistry, Chemistry Department, Faculty of Science, Kasetsart University, Bangkok 10900, Thailand*

[b] *NANOTEC Center of Excellence, National Nanotechnology Center, Kasetsart University, Research and Development Institute, Bangkok 10900, Thailand*

[c] *Department of Chemistry, Université Bordeaux 1, FR-33405 Talence Cedex, France*

ARTICLE INFO

*Article history:*
Received 18 September 2009
Accepted 18 December 2009
Available online 24 December 2009

ABSTRACT

The electron hopping mechanism in the single-walled carbon nanotube (SWCNT)-mediated redox reaction between anthraquinonyl ($AQH_2$) and 4-arylhydroxyl amine (4AHA) groups is studied by density functional theory calculations. The (8, 0) SWCNT is used to mimic the real system of interest. It is found that electrons from the oxidized $AQH_2$ group can be transferred to the oxidizing 4AHA group, at the other end of the nanotube, by a hopping process through the mediating SWCNT. Disparity of electron densities ascribable to non-localized electrons confirms this finding. The disparity, partial electron density difference, and Hirshfeld partial charges analyses show that the SWCNT can hold 87% of the extra electron density of the hypothetical negative intermediate produced from the oxidation of the $AQH_2$ process. Chemical attachments of these two redox reagents to the SWCNT also cause new impurity states within the band gap, thereby giving more metallic characteristics to the system. These findings provide a detailed understanding of the electron hopping process and agree well with a previous experimental study.



## 1. Introduction

Among all nanoscale morphologies of carbon, multi-walled carbon nanotubes (MWCNTs) were first observed under transmission electron microscopy (TEM) by Iijima in 1991 [1]. After that, single-walled carbon nanotubes (SWCNTs) were produced independently by Iijima and Ichihashi [2] and Bethune et al. [3] in 1993. Since these discoveries of low-dimensional carbon nanostructures, carbon nanotubes (CNTs) have attracted much interest in modern nanoscience and nanotechnology due to their novel and structure-dependent properties. Over the years, the physical and chemical properties of CNTs have been well-documented with more and more sophisticated methods. The novel properties of these CNTs allow their application as nanoelectronic devices [4], sensors [5], field emission sources [6], and composite materials [7]. The CNTs also function as nanowires to transport electrons between an electrode and electroactive proteins chemically

* *Corresponding author:* Address: NANOTEC Center of Excellence, National Nanotechnology Center, Kasetsart University, Research and Development Institute, Bangkok 10900, Thailand. Fax: +66 2562 5555x2176.
E-mail address: jumras.l@ku.ac.th (J. Limtrakul).

0008-6223/$ - see front matter © 2009 Elsevier Ltd. All rights reserved.
doi:10.1016/j.carbon.2009.12.049

attached on each end of the tube [8]. The transport distances, controlling the rate of electron transfer, are larger than 150 nm from the enzymatic active center to the electrode [9].

The chemical functionalization reactions for CNTs are categorized into three methods, which are: direct attachment to the graphitic surface, ester linkage, and covalent binding using diazonium reagents with high selectivity. The diazonium media method was further developed by Compton's group to initiate chemisorptions of aryl diazonium salts by direct reduction with hypophosphorous acid in the presence of carbon powder [10–12]. The method was further extended to the application on MWCNTs with anthraquinone-1-diazonium chloride and 4-nitrobenzenediazonium tetrafluoroborate, resulting in the synthesis of 1-anthraquinonyl–MWCNTs (AQ–MWCNTs) and 4-nitrophenyl–MWCNTs (NB–MWCNTs) [13].

Recently, Wong and Compton [14] reported a redox reaction on the same MWCNT for the first time. This MWCNT is functionalized with two redox-active species, directly attached by the diazonium salt method. The 4-arylhydroxyl amine (4AHA) and $AQH_2$ species are generated in the first oxidation cycle from $NO_2$–$C_6H_4$-MWCNT and AQ–MWCNT, respectively. This redox reaction consists of a reversible oxidation and an irreversible reduction; it is studied by the cyclic voltammetry technique. These authors proposed a redox reaction mechanism where $AQH_2$ is the oxidizing agent with the oxidation peak at $E_a = -0.385$ V while NHOH–$C_6H_4$ is the reducing group lessening the oxidation peak at $E_a = 0.125$ V

$$AQH_2\text{–MWCNT–}C_6H_4\text{–NHOH} \rightarrow AQ\text{–MWCNT–}C_6H_4\text{–}NH_2 + H_2O$$

The pathway of electron transfer from $AQH_2$ to the 4-arylhydroxyl amine group is investigated to determine whether it is via intermolecular electron tunneling between reagents or by electron hopping via the CNT. The hopping was proposed to be more favorable because of the shorter distance through the tube compared to a process through the solvent. This phenomenon is unique for both oxidizing and reducing groups confined to the same CNT.

Here, we report a theoretical study on the possible processes of electron hopping between two redox reagents functionalized on the same CNT. The mediating MWCNT (in the real system) is simplified to a semiconducting SWCNT for computational efficiency. Periodic calculations are performed to obtain computed electronic properties as realistic as possible. Although time-dependent calculations can yield more details about the electron transfer, such calculations are not practicable for such a large system due to computational limitations. We have thus limited ourselves to static calculation and have tried to overcome the limitations by focusing on six hypothetical subsystems, using static analysis techniques such as the disparity of the electron densities and the nucleophilic Fukui function plot. This yields enough information to establish and characterize the electron transfer process in the whole system.

We also focus only on the redox reaction and not on the chemical attachment and the preparation steps. Thus, the following redox reaction from $AQH_2$–SWCNT–4AHA, terminated at AQ–SWCNT–4AA, is proposed. It can be subdivided into a reversible oxidation and an irreversible reduction (see Fig. 1), where 4-arylamine is noted as 4AA.

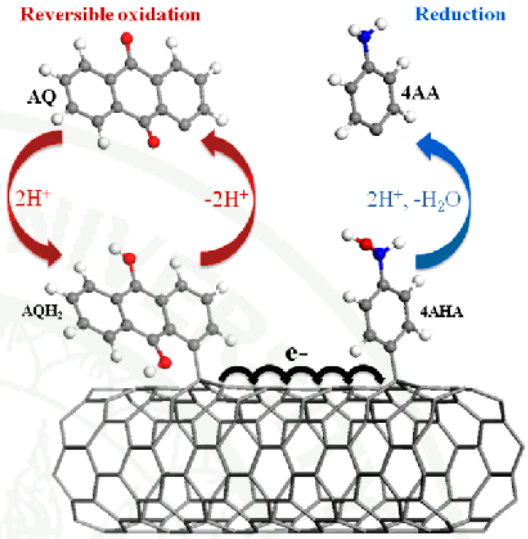


**Fig. 1 – Proposed mechanism for the SWCNT-mediated redox reaction, consisting of a reversible oxidation and an irreversible reduction. The SWCNT accepts electrons from the $AQH_2$ species and donates the electrons to the 4-arylhydroxyl amine.**

*Total reaction:*

$$AQH_2\text{–SWCNT–4AHA} \rightarrow AQ\text{–SWCNT–4AA} + H_2O$$

*Oxidation:*

$$AQH_2\text{–SWCNT–4AHA} \leftrightarrow AQ\text{–SWCNT–4AHA} + 2H^+ + 2e^-$$

*Reduction:*

$$AQ\text{–SWCNT–4AHA} + 2H^+ + 2e^- \rightarrow AQ\text{–SWCNT–4AA} + H_2O$$

## 2. Calibration of the SWCNTs and computational method

The periodic calculations were carried out using the density functional theory (DFT) method as implemented in the DMol3 package [15,16]. For all functionals that we investigated, the generalized gradient approximation (GGA) and an all-electron double numerical basis set with polarized function (DNP) were chosen for these spin-unrestricted computations. These functionals can be applied to large periodic systems and are known to bring about reliable qualitative results. The density functionals used in this work do not include dispersion energy contributions. The DNP basis set corresponds to a double-$\zeta$ quality basis set with a p-type polarization function added to hydrogen and d-type polarization functions added to heavier atoms, and is comparable to 6-31G** Gaussian basis sets, providing a better accuracy, particularly for the hydrogen removal step. The real space global cutoff radius was set to be 3.70 Å. For the geometrical optimizations, all atoms were fully optimized until all the forces on the atoms were less than 0.05 eV $Å^{-1}$. The Brillouin zone was sampled using the Monkhorst–Pack scheme [17].

### 2.1. Calibration of the SWCNTs

In the present approach, a suitably calibrated SWCNT is used to mimic the multi-walled tubes used in the experiments for the computations. The important feature is that the MWCNTs used in the experiments have electronic band gaps like semiconductors. The criterion for the calibration is thus, that the gap of the model-tube should be in the range of 0.5–1.5 eV [18]. The calibration is started with a study of naked ($n$, 0) zigzag SWCNTs, investigated with three functionals and comparing the energy gaps ($E_{gap}$) with each other and with the ones obtained in previous studies. Each initial structure is generated in a supercell periodic box of $20 \times 20 \times 8.52$ Å$^3$, composed of two repeated unit cells of SWCNT along the tube axis. The closest distance between two neighboring SWCNTs is larger than 10 Å in order to be able to ignore intertube interactions in the calculations.

The calibrations are performed in the GGA in the Perdew–Burke–Ernzerhof (PBE) [19], Becke's exchange and Lee, Yang, and Parr's correlation functional (BLYP) [20,21], and non-local exchange–correlation functional (PW91) [22] with the maximum $k$ points of $1 \times 1 \times 50$. The BLYP method is immediately disqualified due to its large average deviation of ±0.079 eV in $E_{gap}$ compared to previous theoretical data [23–28]. The PBE and PW91 methods give the same $E_{gap}$ within a small deviation of ±0.007 eV and a smaller deviation of ±0.044 eV compared to the same data. Although these two methods are very similar, the PBE functional is chosen in our calculations, following the recent theoretical studies [29,30] of periodic systems.

The diameter of the zigzag SWNCTs is then varied systematically and the band gaps studied with the same procedure to find the smallest nanotube representative of the experimental system. Three ($n$, 0) SWCNTs with $n$ mod 3 = 0 are found to be metallic, obeying the empirical ($n$, $n + 3i$) rule for metallic carbon nanotubes, also known as the 1/3 rule: (6, 0) with an $E_{gap}$ of 0.00 eV ($E_{gap,\,calc}$ = 0.00 eV, Ref. [23]); (9, 0) with an $E_{gap}$ of 0.17 eV ($E_{gap,\,expt}$ = 0.080 ± 0.005 eV, Ref. [24] and $E_{gap,\,calc}$ = 0.17 eV, Ref. [25]); and (12, 0) with an $E_{gap}$ of 0.14 eV ($E_{gap,\,expt}$ = 0.042 ± 0.004 eV, Ref. [24] and $E_{gap,\,calc}$ = 0.078 eV, Ref. [23]) (where *expt* is experimental data, *calc* is theoretical data, and $i$ is an integer). The (7, 0) SWCNT also presents a metallic character with an 0.15 eV energy gap (0.21 eV, Ref. [26] and 0.19 eV, Ref. [27]). Thus, the (6, 0), (7, 0), (9, 0), and (12, 0) SWCNTs are certainly not usable as models because of their metallic character.

The (8, 0) SWCNT is found to be the smallest zigzag carbon nanotube that displays a semiconducting behavior with an acceptable energy gap of 0.62 eV. The calculated value is in good agreement with previous data for the $E_{gap}$ (0.643 eV, Ref. [23]; 0.62 eV, Ref. [25]; 0.59 eV, Ref. [27]; and 0.63 eV, Ref. [28]) and confirms that the $E_{gap}$ of $n$ mod 3 = 2 tubes is larger than that $n$ mod 3 = 1 [27]. In order to be able to neglect the intermolecular interaction between the two redox species, the six repeated unit cells along the z-direction of the carbon nanotube are used for the calculations of functionalized tubes. Therefore, the SWCNT-mediated redox models in this work are generated from the validated (8, 0) SWCNT and calculated by periodic calculations with the PBE method.

### 2.2. Redox systems

As seen above, an (8, 0) SWCNT is chosen. For the full redox system, it is functionalized by two redox groups more than 12 Å apart from each other to minimize, and eventually neglect, the intermolecular interaction between these two species. A supercell with $40 \times 40 \times 24.15$ Å$^3$, comprising six periodic lengths for the zigzag SWCNT, is adopted in the calculation with the PBE function (see Fig. S3(a)). Each supercell contains two redox groups, which are covalently bonded to the sidewall of the SWCNT. The smallest distance between two neighboring SWCNTs is larger than 30 Å. In order to save computational time, the $k$ points are reduced to be $1 \times 1 \times 10$, following the previous study [30], to calculate the electronic properties of the full redox system. Only the $\Gamma$ point in the Brillouin zone is also considered for the geometric optimization and orbital analysis.

Even though the individual processes in the overall redox reaction take place concurrently, we simplify the problem by dividing the full redox pathway into six hypothetical states (see Fig. S1), which are: $AQH_2$–SWCNT–4AHA (substrate: *subs*), $[AQH–SWCNT–4AHA]^{1-}$ (*intermediate-1*), $[AQ–SWCNT–4AHA]^{2-}$ (*intermediate-2*: *int-2*), $[AQ–SWCNT–Ph–NH]^{1-}$ (intermediate-3: *int-3*) and AQ–SWCNT–4AA (product: *prod*) (AQ = anthraquinonyl, 4AHA = 4-arylhydroxyl amine, 4AA = 4-arylamine, SWCNT = (8, 0) zigzag SWCNT). The intermediate-1 state can be considered in two configurations, which are termed intermediate-1-a (*int-1-a*) and intermediate-1-b (*int-1-b*) for the removal of H*a* and H*b*, respectively.

Mimicking a half-cell redox reaction, the singly functionalized tubes with two electrons from the oxidation reaction, $[AQ–SWCNT]^{2-}$ (*AQ-tube*) and $[4AHA–SWCNT]^{2-}$ (*4AHA-tube*), are also investigated to consider the possibility of the transfer of these electrons (see Fig. S2). This half-cell redox system is optimized and investigated using the same parameter as the full redox system described above.

## 3. Results and discussion

The diazonium method provides a well-defined chemical bond between the molecule and a carbon atom of the tube rather than the less well-defined interaction between an entire group and the tube surface found in the adsorption of π-conjugated molecules. Indeed, the optimized geometry of the functionalized SWCNTs in the full redox system shows that the reacting groups with closing carbon atoms of the nanotube change their geometries with an average displacement of 0.19 Å for the AQ derivatives and 0.22 Å for the 4AHA derivatives. While the remaining atoms, which are far from the reacting species, of the tube remain roughly at the same positions within, on an average, 0.06 Å. These averages are calculated for all atoms of a desired part changing their relative positions in each step of the mechanism. We also found that the phenyl plane of the 4AHA group (including its derivatives: Ph–NH, and 4AA) is parallel to the perpendicular axis (reference line), which is vertical to the tube axis of the SWCNT medium, as shown in Fig. S4. The angle between the anthraquinonyl plane of the $AQH_2$ group in *subs* and the reference line is sharp, about 30°, due to the steric effect to

the adjacent hydrogen atom (*Hb*) of the hydroxyl moiety of the $AQH_2$ group (see Fig. S3(a)). Whenever this hydrogen atom is cleaved, the repulsive force on the ketone becomes smaller. Thus, a less sharp angle is found, about 10°. However, the AQ group is not exactly sharp to the reference line, because the carbonyl oxygen atom is a hindrance for such an orientation.

The electronic properties of the redox systems are reported in Table 1. The results show that the two configurations of intermediate-1 have relative energy which differs by −0.95 kcal $mol^{-1}$, the *int-1-b* being more favorable than *int-1-a* due to a smaller steric effect between the hydrogen atom of the AQH group (*Hb*) and the nanotube. The proposed mechanism pathway of the redox reaction through *int-2* is presented in snapshots. It starts from the *subs* configuration and goes through *int-1-b*, *int-2*, and *int-3* to *prod*. In more detail: The O–H*b* of the *subs* is first cleaved, as demonstrated in the *int-1-b*, with one electron remaining. Sequentially, the O–H*a* is removed, resulting in the *int-2*. This is a half-cell redox reaction, with, overall, two electrons left. The *int-3* is an intermediate state, corresponding to the *int-2* to *prod* reduction, where a hydroxyl group of the 4AHA is dehydrated by an acidic proton addition, and the Ph–NH group remains. The nucleophilic nitrogen atom of the *int-3* is then also attacked by another electrophilic proton, resulting in the *prod* configuration. The reduction reaction cannot be reversible: A negative −0.26*e* local Hirshfeld charge is found on the nucleophilic nitrogen atom of the Ph–NH part of *int-3*. This makes an attack between this site and an oxygen atom of water highly unlikely.

The chemical attachment of the two redox reagents to the SWCNT creates new impurity states within the band gap. From the pristine SWCNT, $E_{gap}$ = 0.62 eV, the band gap in the redox systems is lowered to less than 0.16 eV, thereby introducing a more metallic character to the system. This eases electron delocalization in the modified system. The electron density difference and Hirshfeld partial charges analyses show that the tube can hold 87% of the extra electron density of the hypothetical negative intermediate produced from the oxidation of the $AQH_2$ (see entry 5 in Table 1). In addition, the remaining charge at the AQ in the *int-2* is −0.19*e*, leading to a reverse reduction of the AQ to the $AQH_2$.

The frontier molecular orbitals of the redox system are illustrated in Fig. S5. An electron ionization and reception occurs at the SWCNT, which can be clearly observed at both the HOMO and LUMO for the substrate. In the intermediate steps, an electronic connection between the AQ and the 4AHA molecules is clearly shown at the HOMO level. An electron movement is proposed as a theoretical mechanism pathway. The first electron from the oxidation reaction of the $AQH_2$ to AQH is initially excited to occupy the LUMO level of the *int-1-b*. In this state, both the AQ group and the nanotube are occupied, as shown in the LUMO level in Fig. S5(b). After that, the second electron is generated from the oxidation of the AQH to AQ, resulting in two excited electrons occupying strongly only in the AQ part in the LUMO level of the *int-2*. This case confirms the reversible reaction of the AQ to $AQH_2$. These two electrons then transfer to the 4AHA part, resulting in the strong occupation in the 4AHA side (Ph–NH) as shown in the LUMO level in Fig. S5(d). The Ph–NH group is eventually reduced by the extra electron at that level, resulting in the 4AA. The HOMO of the *prod* shows that the electrons are distributed mostly at the 4AA and no longer occupy the AQ side. In addition, an electron in the *int-1-b* and *int-2*, which is strongly localized at the AQ part, confirms that it can reversely reduce. This is the reduction reaction from AQ to $AQH_2$. On the other hand, an electron is rarely available at the 4AHA group (Ph–NH) in the *int-2* and *int-3*, leading to an irreversible reduction.

The plots of the difference of the Hirshfeld charge are presented in Fig. 2(a). These plots are calculated from the difference of each atomic charge between the negatively-charged structure and its neutralized version, neglecting relaxations, resulting in the charge difference of the negative atomic charge. An electron in the intermediate states has a high probability of presence at the AQH, leading to the reverse reduction of AQH to $AQH_2$. Two electrons in the *int-2* step have high probabilities at the AQ, 4AHA, and at the bridge in the nanotube, as shown in Fig. 2(a)-2. Therefore, it is clearly verified that the AQ and 4AHA groups can be reduced to $AQH_2$ and 4AA, respectively.

Fig. 2(b) shows the calculated disparity of the electron densities, following the definition; $\Delta\rho(\mathbf{i} \rightarrow \mathbf{j}) = \rho(\mathbf{j}) - \rho(\mathbf{i})$, where $\Delta\rho(\mathbf{i} \rightarrow \mathbf{j})$ is the change of negative charge densities between the negatively-charged structure, $\rho(\mathbf{j})$, and its neutralized version, $\rho(\mathbf{i})$, resulting in the density of only the negative charge. This plot clearly shows the connection between the reducing

**Table 1 – Hirshfeld partial charge (in elementary changes *e*), energy gap (eV), and relative energy (kcal $mol^{-1}$) calculated with the PBE method and DNP basis set for pristine SWCNT, substrate, intermediate, product, and single-functionalized systems (D = direct, I = indirect energy gap).**

| Entry | Structure | Hirshfeld charge | | | | Energy gap (eV) | Relative energy (kcal $mol^{-1}$) |
|---|---|---|---|---|---|---|---|
| | | Partial charge | | | Total | | |
| 1 | Pristine SWCNT | – | – | – | – | 0.62 D | – |
| 2 | Substrate | $AQH_2$ = 0.05 | SWCNT = −0.07 | 4AHA = 0.03 | 0.01 | 0.00 | – |
| 3 | Intermediate-1-a | AQH = −0.06 | SWCNT = −0.91 | 4AHA = −0.02 | −0.99 | 0.04 D | 0.00 |
| 4 | Intermediate-1-b | AQH = −0.16 | SWCNT = −0.81 | 4AHA = −0.02 | −0.99 | 0.04 I | −0.95 |
| 5 | Intermediate-2 | AQ = −0.19 | SWCNT = −1.73 | 4AHA = −0.07 | −1.99 | 0.10 I | – |
| 6 | Intermediate-3 | AQ = −0.07 | SWCNT = −0.77 | Ph–NH = −0.16 | −1.00 | 0.16 I | – |
| 7 | Product | AQ = −0.01 | SWCNT = −0.03 | 4AA = 0.05 | 0.01 | 0.00 | – |
| 8 | $[AQ–SWCNT]^{2-}$ | AQ = −0.27 | SWCNT = −1.72 | – | −1.99 | 0.00 | – |
| 9 | $[4AHA–SWCNT]^{2-}$ | – | SWCNT = −1.92 | 4AHA = −0.07 | −1.99 | 0.00 | – |

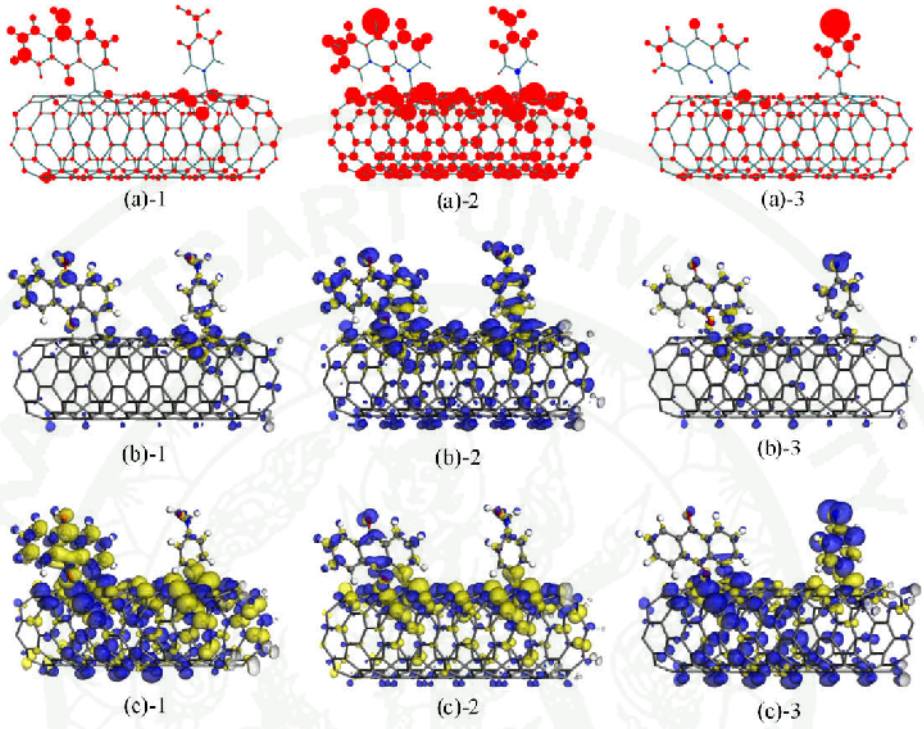


**Fig. 2 – Hirshfeld charge difference (a), where the red color represents a negative charge and the blue color a positive charge. Disparity of electron densities (b), where the blue and yellow colors represent electron accumulation and depression zones, respectively. Nucleophilic Fukui function plot (c). (1 stands for *int-1-b*, 2 for *int-2*, and 3 for *int-3*. (b) and (c) are plotted with an isovalue of ±0.004*e* Å$^{-3}$.) (For interpretation of the references to color in this figure legend, the reader is referred to the web version of this article.)**

group and the oxidizing group. The electron density obviously occupies only the redox molecules and their junction to the SWCNT medium.

The nucleophilic Fukui function plots, as demonstrated in Fig. 2(c), confirm the electron hopping process of the redox reaction via the nanotube. The mechanism starts with a high nucleophilic character of the AQ and its connection. Then, the reducing negative behavior at the AQ leads to an increase at 4AHA. However, the two carbon atoms of the nanotube connected to the AQ and 4AHA species are of the non-conjugated $sp^3$ type. The negative charge density is high at the bridging single bonds of both of the carbon atoms, as depicted in Fig. 2(c)-1–(c)-3, opening a route for the electron transfer from the reducing AQ group to the other. Therefore, the electron transfer between two redox groups can occur by electron hopping via the SWCNT.

The partial electron density difference plots, as shown in Fig. 3, are calculated from the difference of the electron densities between the whole structure and its three divided parts, which are an AQ derivative, a 4AHA derivative, and the tube. The definition; $\Delta\rho(\mathbf{R}) = \rho(\mathbf{R}) - \rho(\mathbf{o}) - \rho(\mathbf{r}) - \rho(\mathbf{m})$ (where $\Delta\rho(\mathbf{R})$ is the partial electron density difference of the redox system; **R** is all redox parts, **o** is the oxidation part, **r** is the reduction part, and **m** is the medium part) is considered and implied to both resonance character and an electron transferable of the system. The plot of *int-1-b* in Fig. 3(b) shows a high electron resonance of the $\pi$-conjugated system, covering the electron transfer, after the H*b* is cleaved. In Fig. 3(a) and (e), the electron transfer is observed between the two functionalized groups and the tube, confirming the electron movement possibility. The electron transfer between two redox groups is shown as the linkage at the tube in *int-2* and *int-3*.

In order to show that both functionalized groups must indeed be present on the same tube, the electron transfer of the singly functionalized tubes (known as the half-cell redox system), the *AQ-tube* and the *4AHA-tube*, is calculated and compared to the full redox system. The Hirshfeld partial charges analyses show that the charge density on the tube is virtually the same in the *AQ-tube* (−1.72*e*) and in the full redox system (−1.73*e*), which eases comparison: a more negative charge is left on the AQ group in the single-functionalized tube due to the lack of further electron accepting groups. When the accepting group, 4AHA, is added to the *AQ-tube* to obtain the full redox system, the remaining electron density in the AQ group is lowered by 30% and donated to the 4AHA (see entries 5 and 8 in Table 1). The plots of the deviation of electron densities of these single-functionalized systems are presented in Fig. S6. The plots show that an electron from the single AQ can transfer to the tube in the *AQ-tube*; and an electron in the tube can also transfer to the single 4AHA group in

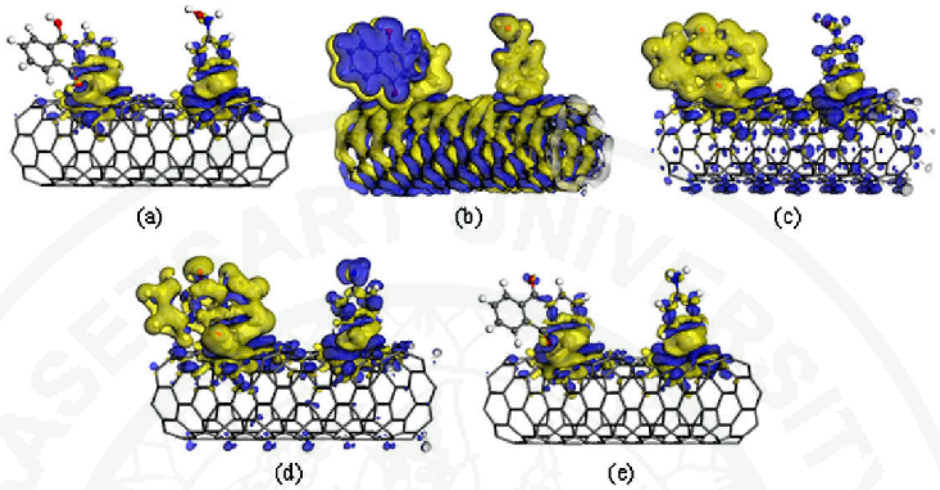


**Fig. 3 – Partial electron density difference of *subs* (a), *int-1-b* (b), *int-2* (c), *int-3* (d), and *prod* (e), plotted for an isovalue of ±0.004*e* Å$^{-3}$.**

the *4AHA-tube*. Two electrons in both singly functionalized systems have high probabilities along the tube, but the electronic junction can be observed only in the full redox system, as described above.

## 4. Conclusions

DFT calculations with the PBE functional are used to investigate the reaction mechanism of electron hopping in the SWCNT-mediated redox reaction of anthraquinonyl ($AQH_2$) and 4-arylhydroxyl amine (4AHA) groups. Our findings can be summarized into three main points. First, the disparity of electron densities, partial electron density difference, and Hirshfeld partial charges analysis show that the SWCNT can hold 87% of the extra electron density of the hypothetical negative intermediate produced from the oxidation of $AQH_2$. Second, the chemical attachment of these two redox reagents to the SWCNT also causes new impurity states to appear within the band gap, thereby introducing a more metallic character to the system. Third, the electrons from the oxidized $AQH_2$ group can be transferred to the oxidizing 4AHA group at the other end of the nanotube by a hopping process through the mediating SWCNT. This mechanism is confirmed by the non-localized distribution of the hopping excited electrons. These findings provide a detailed understanding of the electron hopping process and agree well with previous experimental study. This work is not only complementing experimental study by giving an interpretation in terms of electronic wave functions, but also demonstrates a promising application of the CNT materials in the nanotechnology field.

## Acknowledgements

This work was supported in part by Grants from the National Science and Technology Development Agency (2009 NSTDA Chair Professor funded by the Crown Property Bureau under the Management of the National Science and Technology Development Agency and NANOTEC Center of Excellence funded by the National Nanotechnology Center), Kasetsart University Research and Development Institute (KURDI), the Thailand Research Fund (TRF), and the Commission of Higher Education, Ministry of Education under Postgraduate Education and Research Programs in Petroleum and Petrochemicals and Advanced Materials and the Development and Promotion of Science and Technology Talents Project (DPST). The Kasetsart University Graduate School is also acknowledged. PAB particularly thanks the TRF and NSTDA Chair Professor for the generous support of his visits to Thailand and the Memorandum of Understanding between Kasetsart and Bordeaux 1 Universities. The computational calculations are supported by the Thai National Grid Center (TNGC) under the Software Industry Promotion Agency (SIPA).

## Appendix A. Supplementary data

Supplementary data associated with this article can be found, in the online version, at doi:10.1016/j.carbon.2009.12.049.

REFERENCES

[1] Iijima S. Helical microtubules of graphitic carbon. Nature 1991;354(6348):56–8.
[2] Iijima S, Ichihashi T. Single-shell carbon nanotubes of 1-nm diameter. Nature 1993;363(6430):603–5.
[3] Bethune DS, Klang CH, de Vries MS, Gorman G, Savoy R, Vazquez J, et al. Cobalt-catalysed growth of carbon nanotubes with single-atomic-layer walls. Nature 1993;363(6430):605–7.
[4] Tans SJ, Verschueren ARM, Dekker C. Room-temperature transistor based on a single carbon nanotube. Nature 1998;393(6680):49–52.
[5] Kong J, Franklin NR, Zhou C, Chapline MG, Peng S, Cho K, et al. Nanotube molecular wires as chemical sensors. Science 2000;287(5453):622–5.

[6] de Heer WA, Châtelain A, Ugarte D. A carbon nanotube field-emission electron source. Science 1995;270(5239):1179–80.
[7] Baughman RH, Zakhidov AA, de Heer WA. Carbon nanotubes – the route toward applications. Science 2002;297(5582):787–92.
[8] Gooding JJ, Wibowo R, Liu JQ, Yang W, Losic D, Orbons S, et al. Protein electrochemistry using aligned carbon nanotube arrays. J Am Chem Soc 2003;125(30):9006–7.
[9] Patolsky F, Weizmann Y, Willner I. Long-range electrical contacting of redox enzymes by SWCNT connectors. Angew Chem Int Edit 2004;43(16):2113–7.
[10] Pandurangappa M, Lawrence NS, Compton RG. Homogeneous chemical derivatisation of carbon particles: a novel method for funtionalising carbon surfaces. Analyst 2002;127(12):1568–71.
[11] Wildgoose GG, Pandurangappa M, Lawrence NS, Jiang L, Jones TGJ, Compton RG. Anthraquinone-derivatised carbon powder: reagentless voltammetric pH electrodes. Talanta 2003;60(5):887–93.
[12] Leventis HC, Streeter I, Wildgoose GG, Lawrence NS, Jiang L, Jones TGJ, et al. Derivatised carbon powder electrodes: reagentless pH sensors. Talanta 2004;63(4):1039–51.
[13] Heald CGR, Wildgoose GG, Jiang L, Jones TGJ, Compton RG. Chemical derivatisation of multiwalled carbon nanotubes using diazonium salts. Chem Phys Chem 2004;5(11):1794–9.
[14] Wong ELS, Compton RG. Chemical reaction of reagents covalently confined to a nanotube surface: nanotube-mediated redox chemistry. J Phys Chem C 2008;112(22):8122–6.
[15] Delley B. An all-electron numerical method for solving the local density functional for polyatomic molecules. J Chem Phys 1990;92(1):508–17.
[16] Delley B. From molecules to solids with the DMol$^3$ approach. J Chem Phys 2000;113(18):7756–64.
[17] Monkhorst HJ, Pack JD. Special points for Brillouin-zone integrations. Phys Rev B 1976;13(12):5188.
[18] O'Connell MJ, Bachilo SM, Huffman CB, Moore VC, Strano MS, Haroz EH, et al. Band gap fluorescence from individual single-walled carbon nanotubes. Science 2002;297(5581):593–6.
[19] Perdew JP, Burke K, Ernzerhof M. Generalized gradient approximation made simple. Phys Rev Lett 1996;77(18):3865.
[20] Becke AD. Density-functional exchange-energy approximation with correct asymptotic behavior. Phys Rev A 1988;38(6):3098.
[21] Lee C, Yang W, Parr RG. Development of the Colle–Salvetti correlation-energy formula into a functional of the electron density. Phys Rev B 1988;37(2):785.
[22] Perdew JP, Wang Y. Accurate and simple analytic representation of the electron-gas correlation energy. Phys Rev B 1992;45(23):13244.
[23] Gülseren O, Yildirim T, Ciraci S. Systematic ab initio study of curvature effects in carbon nanotubes. Phys Rev B 2002;65(15):1534051–4.
[24] Ouyang M, Huang JL, Cheung CL, Lieber CM. Energy gaps in "metallic" single-walled carbon nanotubes. Science 2001;292(5517):702–5.
[25] Blase X, Benedict LX, Shirley EL, Louie SG. Hybridization effects and metallicity in small radius carbon nanotubes. Phys Rev Lett 1994;72(12):1878–81.
[26] Zólyomi V, Kürti J. First-principles calculations for the electronic band structures of small diameter single-wall carbon nanotubes. Phys Rev B 2004;70(8).
[27] Valavala PK, Banyai D, Seel M, Pati R. Self-consistent calculations of strain-induced band gap changes in semiconducting ($n$, 0) carbon nanotubes. Phys Rev B 2008;78(23).
[28] Pannopard P, Khongpracha P, Probst M, Limtrakul J. Gas sensing properties of platinum derivatives of single-walled carbon nanotubes: a DFT analysis. J Mol Graph Model 2009;28(1):62–9.
[29] Zhao JX, Ding YH. Chemical functionalization of single-walled carbon nanotubes (SWNTs) by aryl groups: a density functional theory study. J Phys Chem C 2008;112(34):13141–9.
[30] Wu X, Zeng XC. First-principles study of a carbon nanobud. ACS Nano 2008;2(7):1459–65.

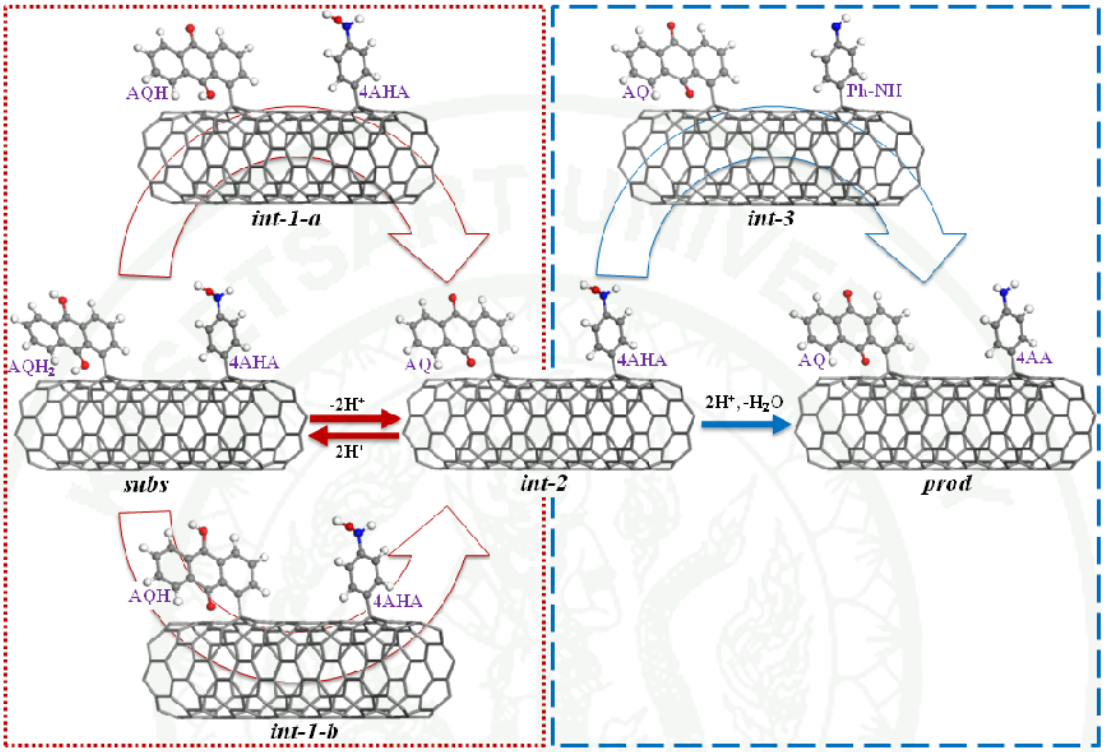

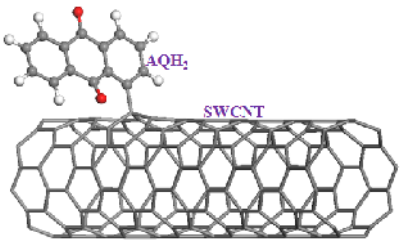


(a)

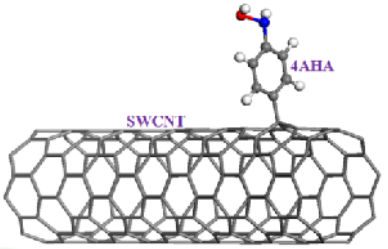


(b)

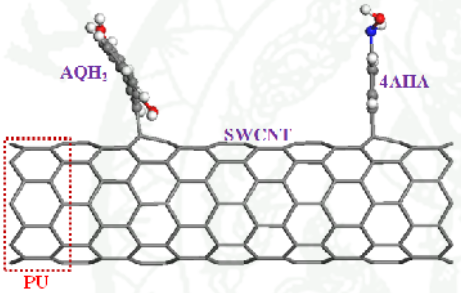


(a)

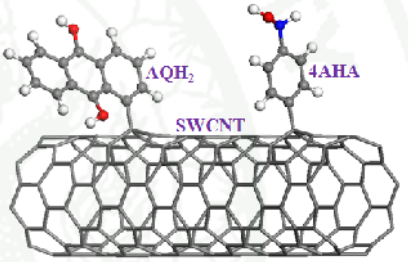


(c)

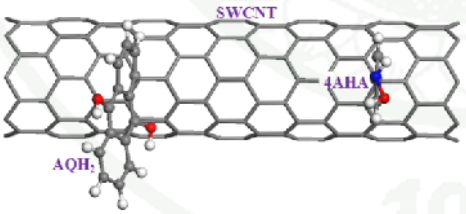


(b)

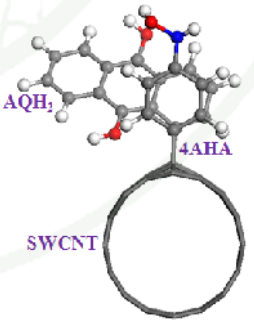


(d)

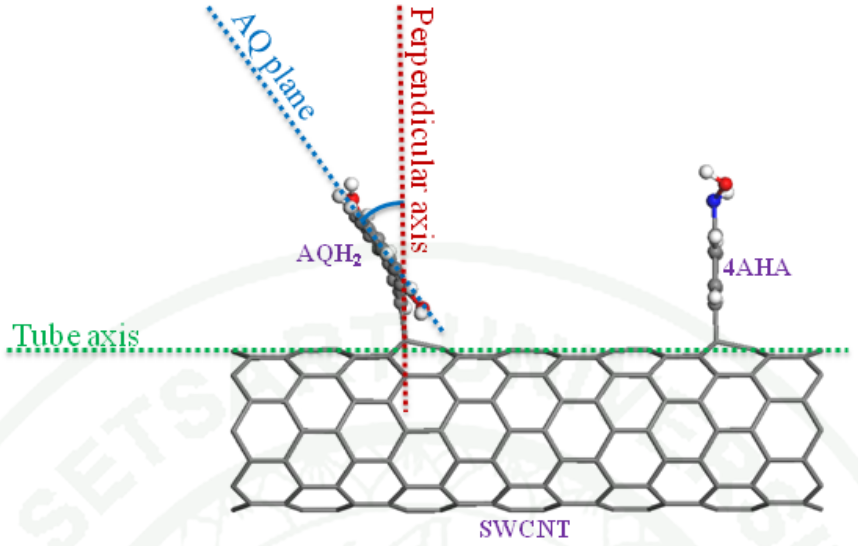

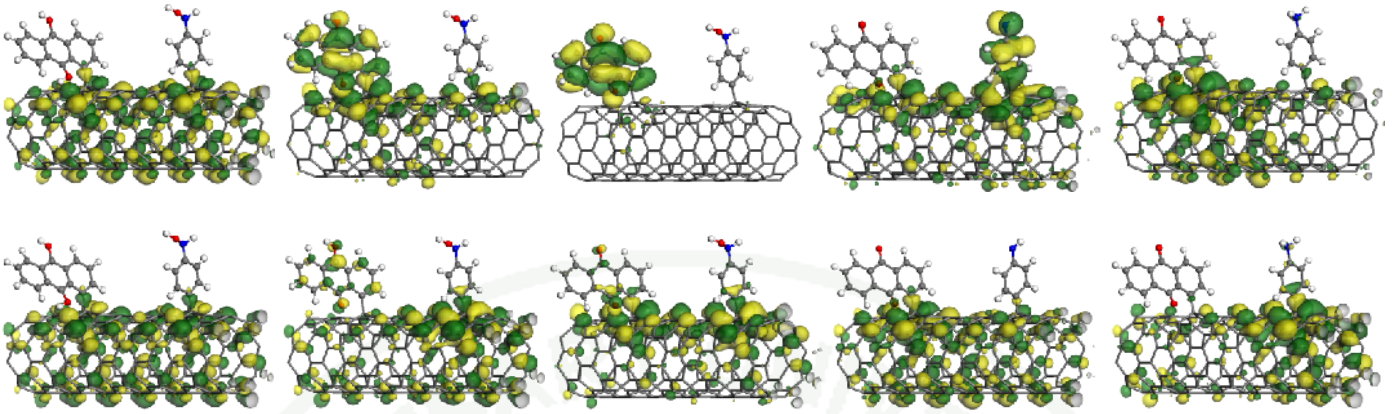

(a) (b) (c) (d) (e)

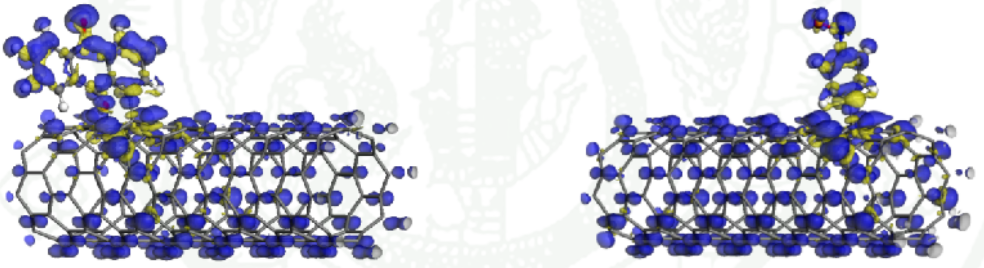

(a) (b)